Production and purification of tagatose with its evaluation in cookie formulations

by

Nilofar Arabi

B.S., University of Tehran, 2024

A THESIS

submitted in partial fulfillment of the requirements for the degree

MASTER OF SCIENCE

Carl and Melinda Helwig Department of Biological and Agricultural Engineering
Carl R. Ice College of Engineering

KANSAS STATE UNIVERSITY
Manhattan, Kansas

2026

Approved by:
Major Professor
Jikai Zhao

Copyright

Abstract

Tagatose is a rare sugar with significant potential as a low-calorie, low-glycemic alternative to conventional sweeteners. The large-scale application of tagatose remains limited by challenges in efficient production and downstream processing. This thesis investigates the production, purification, and functional application of tagatose-rich syrups derived from CaO-promoted isomerization of galactose.

In Chapter 1, a literature review is presented covering the properties, production, and food applications of tagatose. The chapter examines both enzymatic and chemical isomerization routes for converting galactose to tagatose, with particular focus on CaO-promoted alkaline isomerization via the Lobry de Bruyn-van Ekenstein transformation. Downstream purification is reviewed alongside the functional role of tagatose in baked food systems, including its enhanced participation in Maillard browning and its effects on dough rheology and cookie texture. Key knowledge gaps in process integration and food-system performance for tagatose-rich syrups are identified, providing the scientific rationale for the subsequent experimental chapters.

In Chapter 2, the impacts of neutralization strategy (CO_2 vs. H_2SO_4) and ion-exchange resin processing on the purification of tagatose-rich syrups were evaluated. Results demonstrated that neutralization chemistry strongly influences the ionic composition of the feed syrup and, consequently, deionization efficiency. CO_2-neutralized systems exhibited lower initial conductivity and improved ion-exchange performance compared to H_2SO_4-neutralized systems, where residual sulfate ions hindered effective removal. Sequential cation-anion exchange achieved significant reductions in conductivity and divalent ions (Ca^{2+} and Mg^{2+}), producing syrups suitable for food applications. Empirical regression models were developed to relate resin dosage and contact time to conductivity reduction, providing predictive capability for bench-scale process optimization.

In Chapter 3, the functional performance of the purified tagatose-rich syrup was evaluated in shortbread cookie formulations and compared with sucrose and commercial high fructose corn syrup (HFCS). Tagatose-containing formulations exhibited distinct physicochemical behaviors, including increased Maillard browning, altered dough rheology, and differences in moisture retention and texture. Cookies prepared with tagatose syrup showed darker color development, comparable or higher hardness, and modified adhesiveness

relative to sucrose-based systems. This work establishes a systematic framework linking upstream reaction chemistry, downstream purification, and final food functionality. The findings provide critical insights into process optimization, demonstrate the feasibility of producing tagatose-rich syrups, and highlight their potential as functional sugar alternatives in bakery applications.

Table of Contents

List of Figures

List of Tables

Acknowledgements

First, I would like to praise my Lord and Savior, Jesus Christ, for His constant guidance, love, and faithfulness throughout this journey. It was through Him that I found strength in uncertainty and peace in difficult moments. *"Trust in the Lord with all your heart and lean not on your own understanding."* (Proverbs 3:5)

I am deeply grateful to my advisor, Dr. Jikai Zhao, for his guidance, patience, and support throughout my graduate studies. His mentorship helped shape this research and encouraged me to grow as a scientist.

I am also deeply grateful to my family for their unconditional love, support, and encouragement, which have sustained me throughout this process. I would like to sincerely thank my fiancé, Joseph Flippen, and his family for their kindness, patience, and unwavering support. I am truly blessed to have you in my life.

Finally, I would like to thank my best friend, Hediyeh Lakzaei, for her constant support, encouragement, and presence during this journey. Your friendship has meant more to me than words can express.

1 Chapter 1 – Literature Review

1.1 Introduction

Excessive consumption of caloric sweeteners has become a major global health concern over the past several decades.[1] According to the World Health Organization, global sugar intake has increased substantially, with average daily consumption in many developed countries exceeding recommended levels.[2] High dietary sugar intake has been strongly associated with the rising prevalence of metabolic disorders such as obesity, type 2 diabetes, and cardiovascular diseases.[3–5] In the United States, the prevalence of diabetes among adults has more than doubled over recent decades, placing enormous pressure on healthcare systems and motivating the search for effective dietary interventions.[6] These health concerns have driven significant interest in identifying alternative sweeteners that provide desirable sensory properties while reducing caloric intake and glycemic impact.[7]

Among the various candidates, rare sugars have attracted increasing attention due to their unique metabolic characteristics and potential applications in functional foods and nutraceutical formulations.[8–10] Tagatose (it represents the D type for the rest of the thesis) is one of the most promising rare sugars, combining near-sucrose sweetness (approximately 92% relative to sucrose), a substantially lower caloric value (1.5 kcal g^{-1} versus 4 kcal g^{-1} for sucrose), and an extremely low glycemic index (GI ≈ 3), making it particularly attractive for diabetic and low-glycemic diets.[11–13] In addition, tagatose exhibits prebiotic effects and has demonstrated potential benefits in regulating blood glucose levels.[14] These characteristics have generated increasing interest in the food and pharmaceutical industries, yet the widespread adoption of tagatose remains constrained by challenges in efficient and cost-competitive production.

The industrial production of tagatose relies primarily on the isomerization of galactose; an aldose sugar obtained from lactose hydrolysis of dairy byproducts such as whey permeate.[15] Both enzymatic and chemical routes have been developed for this transformation. Enzymatic isomerization using L-arabinose isomerase (L-AI) has demonstrated high selectivity, but faces limitations including poor thermal stability, dependence on metal cofactors, and high enzyme production costs that constrain industrial competitiveness.[16] Chemical

isomerization using CaO, which exploits the selective formation of a $Ca(OH)_2$-tagatose complex intermediate, has emerged as a promising alternative capable of achieving tagatose yields exceeding 70% under ambient conditions.[17,18] However, following isomerization, the reaction mixture contains substantial inorganic ionic loads - primarily calcium, carbonate, or sulfate species depending on the neutralization strategy - that must be systematically removed by downstream purification to achieve higher quality.

Ion-exchange resin purification is the standard approach for demineralization of carbohydrate syrups in industrial food processing and has been applied to sugar solutions.[19] In such systems, cation- and anion-exchange resins selectively remove dissolved salts, metal ions, and residual acid or base species, thereby reducing ionic strength and improving product quality.[20] This step is particularly critical in processes involving chemical isomerization routes, such as CaO-promoted galactose conversion, where significant inorganic species (e.g., calcium, carbonate, or sulfate ions depending on the neutralization pathway) are introduced during reaction and neutralization.[18,21] Effective deionization is therefore essential not only for achieving food-grade standards but also for ensuring desirable physicochemical properties, stability, and downstream functionality of the resulting syrups.[22,23] Consequently, understanding and optimizing ion-exchange purification parameters remains a key aspect of developing scalable and economically viable processes for tagatose-rich syrup production.[12,24]

This thesis addresses these gaps through two interconnected research chapters. Chapter 2 investigates the systematic optimization of CO_2 and H_2SO_4 neutralization routes and ion-exchange resin selection, dosage, and contact time for the purification of CaO-isomerized tagatose-rich syrups and develops empirical regression models to guide bench-scale process design. Chapter 3 evaluates the functional performance of the produced syrup in shortbread cookie formulations compared with sucrose and commercial high fructose corn syrup (HFCS). The present chapter provides the scientific and technological context for this work by reviewing the literature on tagatose properties, production routes, downstream purification strategies, food applications.

1.2 Properties and Health Benefits of Tagatose

Tagatose ($C_6H_{12}O_6$) is a naturally occurring ketohexose and the C-4 epimer of D-fructose. It is found in trace amounts in heat-treated dairy products, some fruits, and cocoa, but at concentrations too low for practical isolation from natural sources.[11] Its water solubility is approximately 58% (w/w) at 20 °C, sufficient for most food and beverage applications.

The most commercially significant attribute of tagatose is its exceptionally low GI compared to 65 for sucrose and 100 for glucose. This arises because only approximately 20% of ingested tagatose is absorbed in the small intestine; the remainder passes to the large intestine, where it undergoes fermentation by resident microbiota.[13] This fermentation profile underpins both the reduced caloric contribution and demonstrated prebiotic activity. Colonic fermentation of tagatose yields short-chain fatty acids, principally butyrate, propionate, and acetate - associated with anti-inflammatory effects and improved intestinal barrier integrity.[25] Clinical studies have documented reductions in HbA1c, improvements in fasting blood glucose, and attenuation of postprandial hyperglycemia following tagatose consumption, attributed to partial inhibition of intestinal sucrase-isomaltase and stimulation of glucagon-like peptide-1 secretion through colonic fermentation.[11]

Beyond its glycemic and prebiotic properties, tagatose is a reducing ketohexose that participates actively in Maillard browning reactions upon heating in the presence of amino compounds.[26] Ketoses such as tagatose react more rapidly in Maillard reactions than aldoses such as glucose or galactose due to differences in Schiff base formation rates and Amadori rearrangement kinetics, resulting in more intense browning at equivalent baking conditions.[27] This property has important implications for the functional performance of tagatose-containing syrups in baked food systems. Tagatose received generally recognized as safe (GRAS) status from the FDA in 2001 following safety evaluations confirming no adverse effects at relevant concentrations and has since been approved as a food ingredient in the United States, European Union, South Korea, Australia, and New Zealand.[28]

1.3 Production of Tagatose from Galactose

The industrial production of tagatose relies on the isomerization of Galactose, which is obtained from

enzymatic hydrolysis of lactose sourced from dairy byproducts, most commonly whey permeates.[15] Lactase (β-galactosidase) cleaves lactose into equimolar quantities of glucose and galactose, and the galactose fraction provides the feedstock for isomerization. Several catalytic strategies have been investigated for this transformation, spanning enzymatic, homogeneous, and heterogeneous chemical systems.

1.3.1 Enzymatic Isomerization

Enzymatic isomerization of galactose to tagatose is catalyzed by L-AI, which accepts galactose and tagatose as substrates due to its broad substrate specificity. L-AI enzymes have been identified from a wide range of organisms including *Lactobacillus* spp., *Bacillus stearothermophilus*, *Thermoanaerobacter mathranii*, and *Caldicellulosiruptor saccharolyticus*.[16,29] Under optimized conditions, L-AI achieves galactose-to-tagatose conversion efficiencies of 50-60%, approaching thermodynamic equilibrium. Thermophilic variants offer higher reaction rates and improved stability but face practical limitations including dependence on divalent metal cofactors (Mn^{2+}, Co^{2+}, Mg^{2+}) that complicate downstream removal, insufficient thermal stability for sustained industrial operation, and high costs of recombinant enzyme production.[16] These constraints have motivated continued development of chemical isomerization approaches.

1.3.2 Chemical Isomerization Using CaO

Chemical isomerization of galactose to tagatose under alkaline conditions proceeds via the Lobry de Bruyn-van Ekenstein (LBAE) transformation, in which aldoses and ketoses are interconverted through a cis-enediol intermediate.[30] Under broadly alkaline conditions, this transformation is non-selective, yielding a complex mixture of monosaccharides through epimerization and retro-aldol fragmentation. The seminal contribution of Beadle, Saunders, and Wajda (U.S. Patents 5,002,612 and 5,078,796) demonstrated that $Ca(OH)_2$ dramatically improves selectivity toward tagatose through the formation of a sparingly soluble $Ca(OH)_2$-tagatose complex intermediate.[18,31] $Ca(OH)_2$ (generated *in situ* by hydration of CaO) forms a selective complex with tagatose that drives equilibrium toward the ketohexose product while simultaneously protecting it from degradation, enabling tagatose yields exceeding 70% at ambient temperature.[17]

The reaction is conducted by dissolving galactose in water and adding CaO at a defined molar ratio (typically

1/1) under stirring at room temperature. The OH^- derived from $Ca(OH)_2$ initiates isomerization by abstracting a proton from the α-carbon of galactose to form a reactive enediol intermediate, while Ca^{2+} coordinates with cis-diol groups on the sugar - particularly at C-1 and C-2 - stabilizing the enediol and facilitating rearrangement to tagatose.[17,32] The $Ca(OH)_2$-tagatose complex is subsequently decomposed by neutralization, releasing free tagatose into solution. Compared to enzymatic routes, this approach offers operational simplicity, ambient-temperature operation, and avoidance of biocatalyst costs, making it well-suited for bench- and pilot-scale development. However, the process introduces substantial inorganic ionic loads (primarily calcium species and CO_3^{2-}, HCO_3^-, or sulfate anions depending on the neutralization route) that must be removed by downstream purification to achieve higher syrup quality.

1.4 Downstream Processing and Purification

1.4.1 Neutralization Strategies

Following CaO-promoted isomerization, neutralization decomposes the $Ca(OH)_2$-tagatose complex and simultaneously precipitates calcium as an insoluble salt. The choice of neutralizing agent is a critical process design decision because it determines the ionic composition of the post-neutralization syrup and therefore governs the performance requirements of downstream ion-exchange purification.

H_2SO_4 generates $CaSO_4$ as the primary precipitate. Due to the low solubility of $CaSO_4$ in water (~2 g L^{-1} at 25 °C), the bulk of the calcium can be removed by filtration. Oroskar et al. (U.S. Patent 9,150,938) explicitly designed their process to avoid ion-exchange deionization by selecting H_2SO_4 neutralization, relying instead on simulated moving bed (SMB) chromatographic separation to recover purified tagatose.[33] However, a fraction of dissolved sulfate ions remains in the clarified syrup due to partial $CaSO_4$ solubility, resulting in a higher and compositionally distinct ionic load that can challenge downstream purification when high-purity syrups are required.

CO_2 is a food-safe alternative that converts dissolved calcium to $CaCO_3$ ($K_S \approx 3.3 \times 10^{-9}$ at 25 °C), readily removed by filtration. Unlike H_2SO_4 neutralization, CO_2 does not introduce exogenous SO_4^{2-} anions into the product stream, yielding a post-neutralization ionic composition dominated by residual carbonate and

bicarbonate species at a lower initial ionic strength.[17] Although ion-exchange deionization cannot be bypassed for CO_2-neutralized syrups, since no filterable low-solubility calcium precipitate is formed, this route avoids sulfate contamination and is more compatible with food-grade processing. The systematic evaluation of CO_2 versus H_2SO_4 neutralization and their effects on downstream ion-exchange performance represents a central focus of Chapter 2.

1.4.2 Ion-Exchange Resin Purification

Ion-exchange resins are cross-linked polymeric materials bearing fixed ionic functional groups that selectively exchange mobile counterions from solutions. Strong-acid cation exchange resins (SAC), bearing sulfonic acid groups in the H^+ form, remove cations such as Ca^{2+}, Mg^{2+}, and Na^+; strong-base anion exchange resins (SBA), bearing quaternary ammonium groups in the OH^- form, remove anions such as SO_4^{2-}, HCO_3^-, and Cl^-. Sequential SAC-SBA two-bed deionization is the standard industrial configuration for producing low-ionic-strength, food-grade carbohydrate syrups.[19,34]

Ion-exchange demineralization is well-established in the production of refined glucose, fructose, and HFCS, where it removes trace minerals, organic acids, and coloring compounds to achieve quality specifications including low ash content and acceptable ICUMSA color.[35] Performance is governed by feed ionic strength, ion valence and hydration energy, resin type and cross-linking, contact time, temperature, and regeneration effectiveness. Divalent cations (Ca^{2+}, Mg^{2+}) are generally removed more efficiently than monovalent cations due to higher charge density. SO_4^{2-} has substantially higher hydration energy than HCO_3^- or CO_3^{2-}, reducing its mobility within resin pores and complicating removal under batch contact conditions. Inadequate regeneration leads to ionic leakage, pH instability, and reduced exchange capacity, compromising product quality.[19]

A specific consideration for galactose-containing syrups is the potential for anion-exchange resins to catalyze isomerization or epimerization under mildly alkaline conditions, as demonstrated by Hashimoto et al., underscoring the importance of resin selection and pH control.[36] Prior studies of ion exchange in enzymatically produced tagatose streams have reported desalination rates above 93% and product purities

suitable for crystallization;[37] however, enzymatic feeds differ substantially in ionic composition from CaO-isomerized feeds, where calcium-rich precipitates and neutralization-derived anions dominate. Performance benchmarks from enzymatic systems cannot be directly transferred to CaO-based routes, establishing a clear need for the systematic process-specific characterization carried out in Chapter 2.

1.5 Functional Properties of Tagatose in Food Systems

1.5.1 Sucrose Functionality in Baked Products

Sucrose is a multifunctional ingredient in baked goods, contributing to bulk and matrix structure, dough rheology, spread during baking, color and flavor development, and moisture retention.[38] In cookie systems, sucrose dissolves in available water and disrupts gluten network formation to produce a tender, short texture; creates a mobile liquid phase during baking that enables lateral flow before the protein-starch network sets; and promotes color and flavor through Maillard reactions between reducing sugars generated by hydrolysis and amino acids from flour protein, as well as through caramelization at elevated temperatures.[38,39] In most cookie formulations, eggs and milk further contribute to this browning by providing proteins rich in lysine and, from milk, lactose as an additional reducing sugar. Even in shortbread, butter introduces small amounts of milk solids that participate similarly.

Sucrose is a non-reducing disaccharide and must first hydrolyze to glucose and fructose before participating in browning, introducing a kinetic delay relative to pre-existing reducing sugars. Recrystallization of sucrose during cooling contributes to the characteristic snap and firmness of shortbread cookies.[39] These interconnected functions make sucrose difficult to replace without compromising product quality.

1.5.2 Alternative Sweeteners in Cookie Formulations

A wide range of sweetener alternatives to sucrose have been evaluated in cookie systems, each with distinct limitations. Liquid sweeteners such as HFCS, invert syrup, and honey provide reducing sugars that promote Maillard browning but differ from sucrose in water-binding behavior, moisture retention, and crystallization potential.[40] HFCS is widely used commercially due to its cost advantage and high reducing sugar content, but its GI is similar to sucrose and it does not improve the nutritional profile of the product.[41] Polyols (sorbitol,

xylitol, erythritol, maltitol) are used in reduced-calorie formulations but generally do not participate in Maillard browning, may introduce cooling sensations, and are associated with laxative effects at high consumption levels.[42,43] High-intensity sweeteners provide sweetness without bulk functional properties and require compensatory bulking agents that may alter texture and color.[44] These limitations motivate the exploration of rare sugars as functionally viable and nutritionally improved sucrose alternatives.

1.5.3 Tagatose in Bakery Systems and Maillard Browning

Rare sugars represent a relatively new category of functional sweeteners in bakery applications. Allulose, as the C-3 epimer of fructose, participates avidly in Maillard browning and produces intense surface browning in baked products even at low substitution levels; its non-metabolizable nature makes it effectively non-caloric and non-glycemic.[8] Tagatose, as a structurally related reducing ketohexose, similarly participates in Maillard browning. Earlier studies in beverage systems documented its thermal stability and identified browning as a key quality consideration at elevated temperatures.[26,45] The Maillard reaction rate is strongly influenced by sugar structure: ketoses react more rapidly than aldoses due to differences in Schiff base formation rates and Amadori rearrangement kinetics.[27] Tagatose has been reported to exhibit higher Maillard browning rates than sucrose, glucose, and galactose in model systems, consistent with the intense surface browning observed in tagatose-containing baked products.[46,47] The Browning Index (BI), derived from CIELAB colorimetric parameters (L*, a*, b*), provides an integrated measure of surface browning intensity used in Chapter 3 to compare browning behavior quantitatively across sweetener systems.[48]

During baking, cookie dough rheology is strongly influenced by the temperature-dependent viscosity of the sugar solution phase, which determines the rate and extent of lateral flow (spread) before the protein-starch network sets.[38] Sugars that produce lower-viscosity liquid phases upon heating promote greater spread; those that produce more viscous phases or participate in earlier structure formation restrict spread and produce thicker, more compact cookies. In terms of moisture, reducing sugars and syrup-based sweeteners exhibit greater affinity for water relative to crystalline sucrose, and are generally associated with higher residual moisture content and softer texture in baked products.[39] The combined influence of tagatose and residual

galactose on these properties in a shortbread cookie system is systematically characterized in Chapter 3.

1.6 Research Gaps and Thesis Objectives

Despite significant progress in understanding Tagatose properties, production chemistry, and potential food applications, several critical knowledge gaps remain. Many reported chemical isomerization systems have been evaluated only in terms of galactose conversion and tagatose yield, without downstream purification. In the CaO-based system specifically, the foundational Beadle et al. patents identify both CO_2 and H_2SO_4 as suitable neutralizing agents but do not characterize the practical differences in ionic composition or downstream deionization requirements that arise from these distinct neutralization chemistries.[17] As the Oroskar et al. patent explicitly chose H_2SO_4 to bypass ion exchange, while CO_2 neutralization makes it essential, a rational design basis for ion-exchange purification of CO_2-neutralized CaO-isomerized syrups is entirely absent from the literature. [33]

In addition, while the properties of highly purified tagatose have been studied in model systems and beverages, the functional performance of a high brix tagatose-rich syrup (containing a mixture of tagatose and residual galactose as produced via CaO-promoted isomerization) in a complex baked food matrix has not been evaluated. The combined influence of tagatose and galactose on dough rheology, cookie spread, color development, texture, and moisture behavior represents a significant knowledge gap for the practical food application of this production route.

Therefore, the specific objectives of this thesis are to systematically evaluate how the choice of neutralization strategy (CO_2 vs. H_2SO_4) and ion-exchange resin selection (type, dosage, and contact time) govern deionization performance and final syrup quality in CaO-isomerized tagatose-rich systems, and to develop empirical regression models to guide bench-scale process optimization (Chapter 2). To assess the functional performance of the produced tagatose-rich syrup in a shortbread cookie system, including dough texture, cookie spread, color development, baked cookie texture, and moisture properties in comparison with sucrose and commercial HFCS under equivalent dry-solids conditions (Chapter 3).

2 Chapter 2 - Purification of Tagatose-Rich Syrup with Ion-exchange Resin Purification

This chapter was adopted from the manuscript: Nilofar Arabi, Seyedamirreza Babaei, Ji Qi, Shubhangi Arvelli, Shaghayegh Janbazialamdari and Jikai Zhao. "Production of Tagatose-Rich Syrup with Ion-Exchange Resin Purification", *Sustainable & Food Technology*.

2.1 Introduction

Tagatose is a rare ketohexose naturally present in trace amounts in dairy products.[49,50] Beyond its nutritional profile, tagatose exhibits prebiotic activity and has demonstrated beneficial effects on blood glucose regulation, dental health, and gut microbiota composition, positioning it as a multifunctional food ingredient rather than a simple sugar substitute.[51–53] Tagatose is produced commercially by isomerization of galactose, which is obtained by hydrolysis of lactose from dairy sources such as whey permeate.[51] Both enzymatic and chemical isomerization routes have been developed. Enzymatic routes using L-AI offer high selectivity and mild conditions, but face challenges related to enzyme cost, thermal instability, and metal ion dependency that constrain industrial competitiveness.[54,55] Chemical isomerization using $Ca(OH)_2$ remains one of the most efficient non-enzymatic routes, capable of achieving tagatose yields exceeding 70% under ambient conditions through the formation of a $Ca(OH)_2$-tagatose complex intermediate that drives the equilibrium toward the ketose product and suppresses sugar degradation.[56] For simplicity, this system is hereafter referred to as CaO-promoted isomerization, reflecting the practical use of CaO, which hydrates in situ to generate $Ca(OH)_2$.

The foundational chemistry of this route was established in seminal patents by Beadle, Saunders, and Wajda, which described the isomerization of galactose to tagatose via a $Ca(OH)_2$-tagatose complex intermediate, followed by neutralization with an inorganic acid or CO_2 to release free tagatose and precipitate calcium salts.[57,58] Those patents explicitly identified a combination of filtration and ion-exchange resin treatment as the necessary downstream steps to remove the resulting inorganic salts and obtain a purifiable tagatose solution, and noted that CO_2, H_2SO_4, HCl, and H_3PO_4 are all suitable neutralizing agents. However, neither patent characterizes how the specific choice of neutralizing agent affects the ionic composition of the post-

neutralization syrup, nor how those differences influence the performance of downstream ion-exchange purification. A more recent patent by Oroskar et al. (U.S. Patent 9,150,938) described a process using $CaO/Ca(OH)_2$ isomerization of galactose from deproteinized whey, followed by H_2SO_4 neutralization, filtration, and SMB chromatographic separation to simultaneously recover pure tagatose and enriched glucose.[59] Notably, this patent explicitly avoids a dedicated ion-exchange deionization step by design: the inventors argued that H_2SO_4 neutralization generates $CaSO_4$ precipitates of sufficiently low solubility to be removed by simple filtration (0.45 μm), making a subsequent ion-exchange stage unnecessary. The patent further noted that when HCl is used instead, the resulting soluble $CaCl_2$ salts cannot be removed by filtration and instead require an expensive ion exchange stage to isolate. This reasoning highlights a critical process-design choice: the feasibility of bypassing ion exchange depends on the neutralizing agent selected and the solubility of the calcium salt it produces. When CO_2 is used for neutralization, which generates carbonate/bicarbonate species rather than sulfate and produces no easily filterable precipitate under mild conditions, the residual ionic load cannot be removed by filtration alone, and ion-exchange deionization becomes essential. Neither the Beadle patents nor the Oroskar et al. patent addresses this scenario, leaving unanswered how CO_2 neutralization governs feed ionic composition or what resin conditions are required to achieve low-ionic-strength syrups from such feeds. Following neutralization, the post-isomerization syrup inevitably contains residual inorganic ions and dissolved salts, including calcium, magnesium, sodium, and anion species, which elevate electrical conductivity and may adversely affect product color, stability, and compliance with food-relevant quality benchmarks.[60,61] The specific ionic profile depends strongly on the neutralizing agent: CO_2 neutralization converts dissolved calcium to $CaCO_3$, leaving primarily carbonate and bicarbonate ions in solution, while H_2SO_4 neutralization generates $CaSO_4$ as the precipitate but leaves a fraction of sulfate ions dissolved due to their partial solubility, resulting in a higher and compositionally distinct ionic load entering downstream purification.[56] In our previous work, CaO-promoted galactose isomerization combined with both CO_2 and H_2SO_4 neutralization yielded clarified tagatose-rich syrups following filtration; however, the dissolved ionic content in both cases remained above conductivity levels

targeted for high-quality syrup production, establishing the need for an additional ion-exchange purification step.[62] Ion-exchange resins are well-established in industrial sugar processing for demineralization, decolorization, and polishing of glucose, fructose, and HFCS streams.[63,64] Sequential strong-acid cation and strong-base anion exchange is the standard configuration for achieving low-ionic-strength, food-compatible syrups, and their performance is strongly dependent on feed composition, resin selection, and operating conditions.[65,66] Ion-exchange polishing has also been applied in enzymatic tagatose production routes. For example, Wen et al. demonstrated that sequential cation-anion exchange beds achieved a desalination rate of 93.8% in an integrated bioprocess for tagatose production from lactose, yielding a syrup of 97.9% purity prior to crystallization.[67] In a related study, ion-exchange chromatography was also employed as the core purification step in a whole-cell biotransformation process for co-production of tagatose and allulose from whey powder.[68] These studies confirm that ion-exchange deionization is a practical purification strategy for tagatose-containing syrups. However, both are based on enzymatic routes in which the ionic composition of the feed entering ion exchange, dominated by metal cofactors, buffer salts, and fermentation-derived species, differs substantially from that generated by CaO-promoted chemical isomerization, where calcium-rich precipitates and neutralization-derived anion species dominate the feed. Performance benchmarks and resin selection criteria established for enzymatic systems therefore cannot be directly transferred to CaO-isomerized feeds. Ion-exchange performance is sensitive to feed ionic strength, ion speciation, resin type, dosage, contact time, and regeneration effectiveness. Inadequate regeneration leads to ionic leakage, pH instability, and reduced exchange capacity, all of which compromise product quality and process consistency.[63] An additional consideration specific to galactose-containing syrups is the potential for anion-exchange resins to catalyze isomerization or epimerization of galactose under alkaline conditions, as recently demonstrated by Hashimoto et al.[69] This underscores the importance of careful resin selection and operating pH control in tagatose-rich systems. Despite the established role of ion exchange in sugar processing and its early identification as a necessary step in CaO-based tagatose production, no systematic study has examined how the choice of neutralization agent governs the ionic composition of the feed entering ion exchange and, in turn, determines

deionization efficiency and final syrup quality. As discussed above, this is not a peripheral question: the Oroskar et al. patent explicitly chose to avoid ion exchange by using H_2SO_4, which produces an easily filtered precipitate. The practical alternative, CO_2 neutralization, which is safer, generates no sulfate residues, and avoids introduction of exogenous anions, produces a fundamentally different ionic environment in which ion-exchange deionization cannot be bypassed. CO_2 and H_2SO_4 neutralization generate different post-neutralization anion distributions, different residual calcium speciation, and different overall ionic strengths, all of which directly affect resin capacity utilization, conductivity reduction efficiency, and the operating conditions required to meet food-relevant quality benchmarks. Characterizing this coupling between neutralization chemistry and ion-exchange performance is therefore essential for establishing a rational process design basis for CaO-isomerized tagatose-rich syrups. Therefore, the objective of this study is to systematically evaluate how the upstream neutralization strategy governs downstream ion-exchange performance in CaO-promoted tagatose-rich systems. By comparing CO_2 and H_2SO_4 neutralization routes across a range of resin combinations, dosages, and contact times, this work aims to identify the key variables controlling deionization efficiency, ionic removal, and syrup quality, and to develop empirical bench-scale operating guidelines that can inform future process development for tagatose-rich syrup production.

2.2 Methods and Materials

2.2.1 Preparation of Tagatose-Rich Feed Syrup

D-(+)-Galactose (≥99%, Sigma-Aldrich, USA) was dissolved in deionized water to prepare a 0.5 M aqueous solution. CaO (Fisher Scientific, USA) was added at a 1/1 molar ratio (CaO/galactose) under continuous stirring at room temperature to initiate alkaline isomerization toward tagatose. Following isomerization, the reaction mixture was neutralized using either CO_2 or H_2SO_4 (Fisher Scientific, USA) to remove excess calcium species. For CO_2 neutralization, the reaction mixture containing the Ca-tagatose gel complex was transferred to a carbonation device (SodaStream International Ltd., United Kingdom), and CO_2 was bubbled through the solution at room temperature for 3-5 min. This step facilitated the conversion of dissolved calcium species to $CaCO_3$, as indicated by visible precipitation and stabilization of pH. For acid neutralization,

concentrated H_2SO_4 was slowly added dropwise under stirring to promote precipitation of calcium sulfate. The formation of precipitates and stabilization of pH suggested effective neutralization, although complete precipitation was not independently verified. Following neutralization, all suspensions were allowed to settle for 30 min and subsequently filtered under a membrane-based vacuum filtration (Corning, Fisher Scientific, USA) to remove $CaCO_3$ or $CaSO_4$ precipitates. The clarified syrup (≈7 °Brix, density 1.028 g mL^{-1}, conductivity ≈ 2.6 mS cm^{-1}, pH ≈ 7) was stored at 4 °C prior to deionization experiments.

2.2.2 Ion-exchange Resins and Regeneration

Four commercial ion-exchange resins (DIAION®, Mitsubishi Chemical, Japan) were evaluated: two strong-acid cation exchangers, PK212 and SK1B (capacity ≈ 1.5 meq mL^{-1}), and two strong-base anion exchangers, PA312 and HPA25L (capacity ≈ 1.2 meq mL^{-1}). Prior to use, all resins were prewashed with deionized water, sieved to remove fines (<100 μm), and regenerated. Cation exchangers were regenerated in 0.5 M HCl and anion exchangers in 0.3 M NaOH by soaking 2 g resin portions in regenerant for 30 min at room temperature. Resins were rinsed repeatedly with deionized water until the effluent conductivity was ≤ 200 μS cm^{-1} and the pH stabilized between 6.5 and 7.0. Successful regeneration was verified by stabilization of rinse conductivity, indicating removal of residual regenerant and attainment of the desired ionic form.

2.2.3 Batch Deionization Experiments

Batch deionization experiments were conducted using 25 mL aliquots of CO_2- or H_2SO_4-neutralized syrup. Batch operation was selected to enable rapid screening of resin combinations and operating conditions prior to column-scale implementation. Each run consisted of sequential cation and anion exchange treatments using the resin combinations listed in **Table 2.1**. For each stage, 2 g of resin were added to the syrup and stirred at 500 rpm and 25 ± 1 °C for 20 min. Resins were removed by vacuum filtration, and conductivity and pH of the filtrates were measured immediately. The cation-treated syrups were transferred to fresh vessels containing regenerated anion resins for a second 20-min treatment under identical conditions. Sugar composition (galactose, tagatose, by-products) was verified by high-performance liquid chromatography (HPLC), and elemental analysis (Ca, Mg, Na, S, Fe, Cu, Mn, As, Pb, Cd, Hg) was quantified by ICP-OES.

Apparent dilution factors were calculated as the ratio of the initial sugar concentration (before deionization) to the corresponding concentration after deionization. All experiments were performed in duplicate.

Table 2.1 Operating conditions for the screening of ion-exchange resin combinations under CO_2- and H_2SO_4-neutralized syrup conditions. All experiments were conducted using a galactose concentration of 0.5 M, a CaO/galactose molar ratio of 1/1, syrup volume of 25 mL, resin mass of 2 g for each resin, contact time of 20 min (for cation) + 20 min (for anion), stirring speed of 500 rpm, temperature of 25 °C, and vacuum filtration for solid removal.

Run No.	Neutralization acid	Cation resin type	Anion resin type
1	CO_2	Cation A	Anion A
2	CO_2	Cation A	Anion B
3	CO_2	Cation B	Anion A
4	CO_2	Cation B	Anion B
5	H_2SO_4	Cation A	Anion A
6	H_2SO_4	Cation A	Anion B
7	H_2SO_4	Cation B	Anion A
8	H_2SO_4	Cation B	Anion B

Cation A= DIAION PK212, Cation B= DIAION SK1B, Anion A= DIAION PA312, Anion B= DIAION HPA25L

2.2.4 Evaporation and Final Syrup Quality Evaluation

Deionized syrup obtained under optimized ion-exchange conditions (7-8 °Brix, conductivity ≈ 250 μS cm^{-1}) was concentrated by controlled vacuum evaporation. Evaporation was carried out using a rotary vacuum evaporator (Büchi R-100, Switzerland) operated at 50 °C and -0.08 MPa until target soluble-solids contents of 65 and 75 °Brix were reached. Duplicate batches (n = 2) were prepared, and samples were collected at two concentration stages, after reaching 65 °Brix and after reaching 75 °Brix, yielding four evaporated syrup samples in total. Following evaporation, syrup samples were stored in sealed containers at 4 °C prior to analysis. Physicochemical and compositional analyses were performed immediately after concentration.

These analyses included color (A_{420} and ICUMSA), water activity, ash content, electrical conductivity, pH, sugar composition (HPLC), and mineral composition (ICP-OES). Microbiological quality was evaluated by total aerobic mesophilic count (TAMC), total yeast and mold count (TYMC), and detection of foodborne pathogens (Escherichia coli, Salmonella spp., and Staphylococcus aureus) in accordance with the FDA Bacteriological Analytical Manual (BAM). Microbiological analyses were conducted after approximately two weeks of refrigerated storage to assess microbial stability of the concentrated syrups under realistic handling and storage conditions.

2.2.5 Analytical Methods

Electrical conductivity and pH were measured at 25 ± 0.5 °C using a calibrated benchtop meter (Sper Scientific, USA). To reduce viscosity-related artifacts associated with high-Brix sugar syrups, conductivity measurements were performed on ten-fold diluted samples prepared with deionized water. These measurements represent method-defined values for comparative purposes and do not correspond to the absolute conductivity of the native concentrated syrups. Soluble-solids content (°Brix) was determined using a digital refractometer (AgTec Portable Refractometer, USA). Water activity (a_w) was measured at 25 °C after a 10 min equilibration period using a water-activity meter (AquaLab 4TE, USA). Sugar compositions (tagatose, galactose, and minor sugars) were quantified by HPLC using an Agilent 1200 HPLC system equipped with a refractive index (RI) detector and a Rezex RPM-Monosaccharide column (Phenomenex, USA). Deionized water was used as the mobile phase at a flow rate of 0.6 mL min^{-1}, and the column temperature was maintained at 80 °C. 5-Hydroxymethylfurfural (HMF) was quantified using an Agilent Technologies 1260 Infinity HPLC system equipped with a UV detector and a Bio-Rad Aminex HPX-87H ion-exclusion column (300 × 7.8 mm). The column temperature was maintained at 65 °C, and 5 mM H_2SO_4 was used as the mobile phase at a flow rate of 0.6 mL min^{-1}. Quantification of tagatose and galactose was performed using external calibration with analytical standards over an appropriate concentration range. Calibration curves exhibited linear responses ($R^2 > 0.99$), and concentrations were determined based on peak area. Analytical accuracy was further evaluated by calculating mass-based sugar recovery across the

deionization step using measured pre- and post-treatment concentrations and corresponding liquid volumes (see Section 3.5); recovery values of 90-113% across all runs confirmed the absence of systematic analytical bias or selective sugar loss during processing. All measurements were conducted in duplicate, and variability between replicates was within acceptable limits. HMF concentrations were quantified using external calibration with standard solutions. Calibration curves exhibited linear detector response, and concentrations were determined based on peak area. Elemental composition (Ca, Mg, Na, S, Fe, Cu, Mn, As, Pb, Cd, Hg) of initial, deionized, and evaporated syrups was determined by ICP-OES (Agilent 5800, USA) following dilution in 2% HNO_3 with external calibration. Ash content was analyzed according to AOAC 923.03 by drying 2-3 g of syrup in porcelain crucibles and ashing at 550 °C for 6 h in a muffle furnace (Thermo Scientific, USA) until constant mass. Color at 420 nm (A_{420}) was measured using a UV-Vis spectrophotometer (Thermo Scientific BioMate 3, USA) with 1 cm quartz cuvettes. For high-solids syrups (65-75 °Bx), absorbance was measured on 10× diluted samples, and ICUMSA color values were calculated according to ICUMSA Method GS2/3-9 (2005).[70]

$$\text{ICUMSA (IU)} = \frac{1000 \times A_{420}}{b \times c} \quad (1)$$

where A_{420} is the color absorbency at 420 nm, b is the optical path length (cm) and c is the concentration of the diluted sample (g mL^{-1}). All analytical measurements were performed in duplicate, and results are reported as mean values.

2.3 Results and Discussion

2.3.1 Galactose Isomerization Performance

Galactose conversion and tagatose selectivity were quantified for each of the eight experimental runs listed in **Table 2.1** following CaO-Promoted isomerization and subsequent neutralization using CO_2 or H_2SO_4 (**Figure 2.1**). Feed syrup preparation followed the protocol established in our previous work, and the resulting conversion and selectivity values were consistent with those previously reported for alkaline CaO-Promoted isomerization systems.[62] Galactose conversion values ranged from approximately 83% for CO_2-neutralized syrups (runs 1-4) to approximately 90% for H_2SO_4-neutralized syrups (runs 5-8), indicating that high

conversion was achieved under both neutralization routes. Similarly, tagatose selectivity values were approximately 53% for CO_2-neutralized feeds and 71% for H_2SO_4-neutralized feeds, remaining within the expected range for base-catalyzed isomerization. Although modest differences in selectivity were observed between the two neutralization routes, both approaches yielded chemically stable and compositionally consistent feed syrups suitable for subsequent deionization and purification studies. The observed difference in selectivity between CO_2- and H_2SO_4-neutralized systems is attributed to differences in the neutralization pathway rather than the formation of chemically distinct products. In both cases, the final product is tagatose. However, sulfuric acid neutralization leads to a rapid quench of the alkaline reaction environment, which can suppress side reactions and result in higher apparent selectivity. In contrast, CO_2 neutralization proceeds through carbonate equilibria and a more gradual pH adjustment, which may allow limited side reactions to occur. While the H_2SO_4-neutralized system exhibits higher selectivity at the reaction stage, it also introduces higher inorganic content, which can increase the ionic load and complicate downstream purification. In contrast, CO_2 neutralization provides a more favorable balance between reaction performance and subsequent deionization.

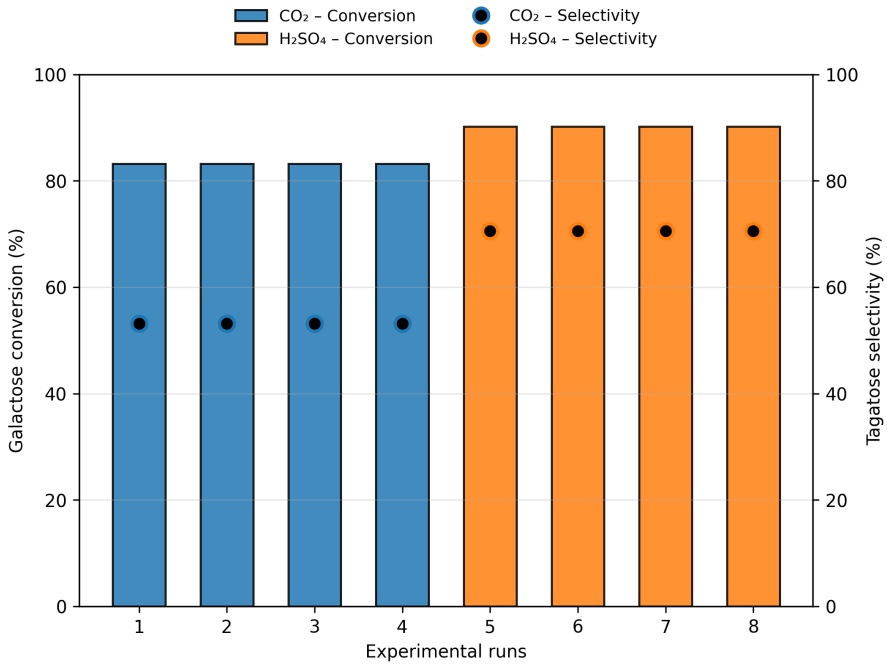

Figure 2.1 Galactose conversion (bars) and tagatose selectivity (circles) following CaO-promoted

isomerization for the eight experimental runs. Values represent the average of duplicate analytical measurements for each feed syrup; identical values across runs reflect the use of the same feed syrup for multiple experimental runs.

2.3.2 Effect of Neutralization Routes on Ionic Conductivity

The conductivity of the tagatose-rich syrup prior to deionization varied markedly with the neutralization route (**Figure 2.2**). Syrups neutralized with CO_2 exhibited an initial conductivity of approximately 2.6 mS cm^{-1}, whereas those neutralized with H_2SO_4 showed a higher value of 3.16 mS cm^{-1}. This difference arises from the distinct ionic species introduced during neutralization: CO_2 neutralization forms soluble HCO_3^- and CO_3^{2-}, whereas H_2SO_4 generates SO_4^{2-} ions that tend to remain dissociated even after partial Ca^{2+} precipitation.[71] Following ion-exchange treatment, the conductivity of all CO_2-neutralized syrups decreased substantially, reaching 262-902 μS cm^{-1}, while H_2SO_4-neutralized syrups showed more variable reductions (442-1728 μS cm^{-1}). The greater ionic strength in the H_2SO_4 system likely resulted from incomplete removal of divalent sulfate salts and slower ion diffusion within the resin pores due to higher ionic density. These findings confirm that the composition of neutralizing agents significantly influences the downstream deionization load and therefore must be optimized prior to large-scale operation. The greater difficulty in removing sulfate from H_2SO_4-neutralized feeds is consistent with the higher hydration energy of SO_4^{2-} relative to HCO_3^-/CO_3^{2-}, which results in stronger competition for resin exchange sites and reduced ion mobility within the resin pores under the batch contact conditions used here; however, direct confirmation of this mechanism would require speciation-resolved analytical measurements beyond the scope of the present study.

2.3.3 Screening of Cation-Anion Resin Combinations and Color Absorbency

The performance of the four cation-anion resin pairs is summarized in **Figure 2.2**, considering both conductivity reduction and A_{420} before and after ion-exchange treatment. For the CO_2-neutralized syrup (Runs 1-4), the untreated feed exhibited conductivities of approximately 2600 μS cm^{-1} with relatively low initial A_{420} (0.045-0.050). Following resin treatment, substantial reductions in conductivity were observed, particularly for the Cation A-Anion A combination (Run 1), which reduced conductivity to 262 μS cm^{-1} and

simultaneously lowered absorbency to 0.020. The Cation A-Anion B system (Run 2) showed a similar trend, reducing conductivity to ≈ 420 µS cm^{-1} with a final absorbency of 0.025. In contrast, systems containing Cation B (Runs 3-4) retained higher residual conductivities (675-902 µS cm^{-1}) and correspondingly higher absorbency values (0.030-0.035), indicating less effective removal of both ionic and colored species. For the H_2SO_4-neutralized syrup (Runs 5-8), the untreated samples exhibited markedly higher conductivities (3160 µS cm^{-1}) and significantly darker color (A_{420} ≈ 0.26), reflecting greater color formation during acid neutralization. After ion exchange, Runs 5 and 6 (Cation A-based systems) reduced conductivity to 442 and 512 µS cm^{-1}, respectively, with absorbency decreasing to ≈ 0.145-0.155. In contrast, systems containing Cation B (Runs 7-8) showed limited conductivity reduction (1598-1728 µS cm^{-1}) and retained higher absorbency (0.21-0.22). Across both neutralization methods, lower final conductivity generally corresponded to lower A_{420} values, indicating that effective ion exchange also promoted partial decolorization. However, the relationship was not strictly linear, suggesting that while removal of inorganic ions contributes to color reduction, additional non-ionic chromophoric compounds remain.

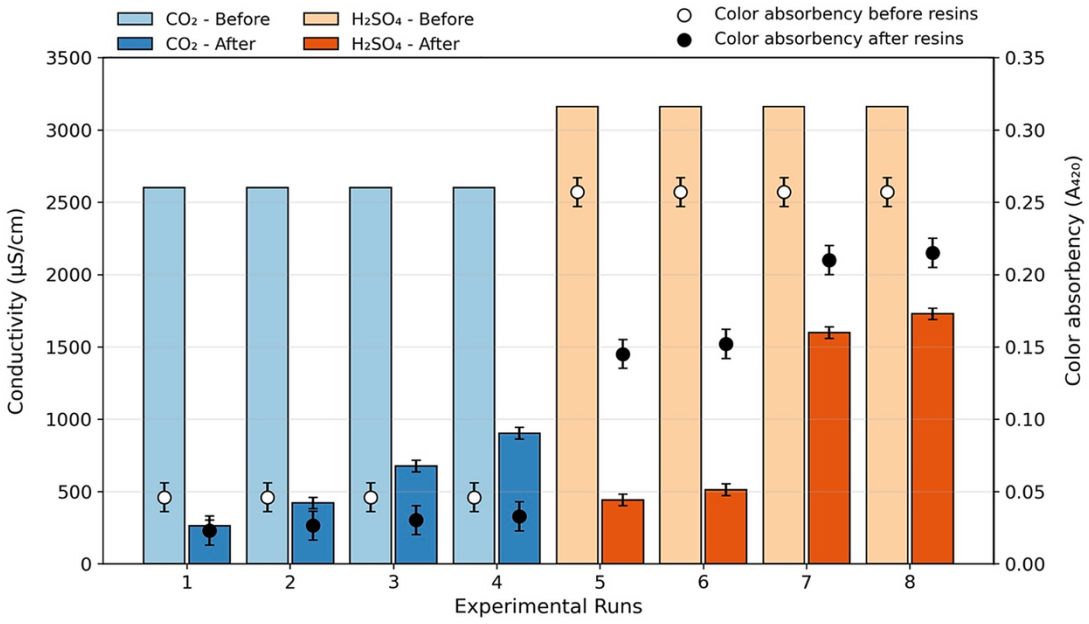

Figure 2.2 Effect of resin treatment on syrup conductivity for CO_2- and H_2SO_4-neutralized tagatose-rich syrups on conductivity and color A_{420} (color-coded by neutralization type). Bars represent mean values of

duplicate measurements, and error bars indicate standard deviations. Initial conductivity values showed no variability across runs and are therefore presented without error bars.

2.3.4 Deionization Performance and Elemental Composition

ICP-OES for the eight experimental runs provided insights into elemental changes during deionization, and the numerical trends broadly followed the conductivity trends observed for each resin-neutralization combination. The untreated CO_2-neutralized syrup (initial sample for Runs 1-4) contained high Ca (813.7 ppm) and moderate Mg (38.2 ppm), consistent with residual calcium originating from the CaO-based isomerization system (**Table 2.2**). Small quantities of sodium (2.1 ppm) were also detected, whereas trace metals such as Fe, Cu, Mn, Pb, As, and Cd were either absent or present only at sub-ppm levels. The presence of these trace elements is attributed to minor impurities in reagents (e.g., CaO and neutralizing agents), residual ions in deionized water, and potential contributions from laboratory equipment or resin materials. The relatively consistent Mg concentration observed in the initial syrup suggests that it primarily originates from the starting materials rather than being introduced from materials used in the process. After ion-exchange treatment, all four CO_2-neutralized runs showed substantial decreases in divalent elements, consistent with effective cation removal (**Table 2.2**). Calcium levels fell to 17-116 ppm depending on the resin pair, corresponding to removal efficiencies of approximately 86-98%. The lowest residual Ca (17-27 ppm) occurred in Runs 1-3, which also achieved the lowest conductivities (262-675 μS cm^{-1}) (**Table 2.2**). Magnesium values similarly decreased from 38.2 ppm to 0.39-11 ppm, demonstrating effective Mg removal across all CO_2-neutralized runs. Sodium increased moderately after treatment (Na 12-29 ppm), which may be associated with resin regeneration chemistry and ion exchange processes. Trace metals remained minimal, with Cu, Mn, As, Pb, and Cd consistently below 0.05 ppm except for Hg (0.09 ppm) and Fe in the initial sample (0.40 ppm). The sulfuric acid-neutralized syrup (initial sample for Runs 5-8) displayed a different elemental profile, with lower Ca (620 ppm), higher Mg (40 ppm), and elevated sulfur (1200 ppm), consistent with the use of sulfuric acid during neutralization (**Table 2.2**). After resin treatment, calcium concentrations decreased only to 57-215 ppm, and magnesium to 4.3-7.2 ppm, indicating less efficient removal of divalent

elements compared with the CO_2-neutralized system (**Table 2.2**). Sodium increased after treatment (15-52 ppm), again reflecting interactions associated with resin operation. Elevated sulfur concentrations persisted in all H_2SO_4-neutralized runs (350-885 ppm), indicating the persistence of sulfur in the system following neutralization and treatment. These results are consistent with the higher post-treatment conductivity observed for acid-neutralized syrups and the greater difficulty in achieving low-ionic-strength conditions. As with the CO_2 system, trace metals (Pb, As, Cd, Hg) remained at very low levels, confirming that the process does not introduce hazardous elemental contaminants. To provide a rigorous basis for assessing ionic removal independently of dilution effects, mass-based removal efficiencies were calculated for Ca, Mg, Na, and S by multiplying measured ICP-OES concentrations by the corresponding liquid volumes. The initial syrup volume was 25 mL for all runs; post-deionization volumes were calculated from the average dilution factor of galactose and tagatose (**Section 2.3.5**), ranging from 28.7 to 45.9 mL. The resulting ion mass balances are summarized in **Table 2.3**. For CO_2-neutralized feeds (Runs 1-4), Ca mass-based removal efficiencies ranged from 83.6% (Run 4) to 97.0% (Run 1). Mg removal ranged from 77.4% to 99.3%. Na mass increased after treatment in all CO_2 runs, consistent with Na^+ leaching from the NaOH-regenerated anion resin, confirming that conductivity reductions reflect cation removal rather than dilution artefacts. Sulfur was not detected in CO_2-neutralized feeds or effluents, consistent with the absence of sulfate in this neutralization pathway. For H_2SO_4-neutralized feeds (Runs 5-8), Ca mass-based removal ranged from 38.4% (Run 7) to 83.8% (Run 5), substantially lower than the CO_2 system due to the competing ionic load of residual dissolved sulfate. Sulfur mass removal ranged from 3.1% (Run 7) to 48.5% (Run 5), demonstrating that batch anion exchange can only partially reduce the sulfate load from H_2SO_4 neutralization. The low Ca and S removals in Run 7 (38.4% and 3.1%, respectively) directly explain its highest residual conductivity (1598 $\mu S\ cm^{-1}$). The apparent negative S removal in Run 8 falls within measurement uncertainty of duplicate ICP-OES determinations and is not interpreted as a net increase.

Table 2.2 Elemental composition of syrups before and after resin treatment (ICP-OES).

Sample	EC (µS cm^{-1})	Ca (ppm)	Mg (ppm)	Na (ppm)	S (ppm)	Fe (ppm)	Cu (ppm)	Mn (ppm)	As (ppm)	Pb (ppm)	Cd (ppm)	Hg (ppm)
Initial syrup for 1-4	2600	813.71	38.22	2.09	N.D.	0.40	N.D.	0.00	N.D.	N.D.	0.00	0.09
Run 1	262	16.83	0.39	12.01	N.D.	N.D.	0.01	0.01	N.D.	N.D.	0.00	0.01
Run 2	420	19.00	1.56	15.6	N.D.	N.D.	0.00	0.01	0.01	N.D.	0.00	0.01
Run 3	675	27.20	2.50	21.00	N.D.	N.D.	0.00	0.03	0.01	N.D.	0.00	0.01
Run 4	902	116.40	11.30	28.64	N.D.	N.D.	0.00	0.00	0.01	N.D.	0.00	0.00
Initial syrup for 5-8	3160	620	40.01	2.32	1200	0.40	N.D.	0.00	N.D.	N.D.	0.00	0.07
Run 5	442	57.12	4.26	15.57	350.58	0.01	0.03	0.20	0.01	N.D.	0.00	0.01
Run 6	512	65.30	4.83	22.07	520.02	N.D.	0.00	0.03	N.D.	N.D.	0.00	0.03
Run 7	1598	214.81	7.18	38.13	654.03	0.12	0.01	0.18	N.D.	N.D.	0.00	0.01
Run 8	1728	82.17	6.01	52.03	884.61	0.30	0.01	0.04	N.D.	0.00	0.00	0.01

N.D. = Not detected. EC = Electrical Conductivity.

Table 2.3 Mass-based ion removal across ion-exchange runs.

Run	**Neutralization acid**	**V_fin (mL)**	**Ca IN (mg)**	**Ca OUT (mg)**	**Ca Rem. (%)**	**S IN (mg)**	**S OUT (mg)**	**S Rem. (%)**
1	CO_2	35.7	0.0203	0.0006	97.0	N.D.	N.D.	N/A
2	CO_2	33.4	0.0203	0.0006	96.9	N.D.	N.D.	N/A
3	CO_2	34.7	0.0203	0.0009	95.4	N.D.	N.D.	N/A
4	CO_2	28.7	0.0203	0.0033	83.6	N.D.	N.D.	N/A
5	H_2SO_4	44.0	0.0155	0.0025	83.8	0.0300	0.0154	48.5
6	H_2SO_4	45.9	0.0155	0.0030	80.7	0.0300	0.0239	20.4
7	H_2SO_4	44.4	0.0155	0.0095	38.4	0.0300	0.0290	3.1
8	H_2SO_4	35.9	0.0155	0.0030	81.0	0.0300	0.0317	−5.7

N.D. = not detected.

2.3.5 Sugar Composition After Deionization

To assess whether ion-exchange deionization selectively removed or transformed either sugar, absolute masses of galactose and tagatose were calculated before and after resin treatment by multiplying HPLC-measured concentrations (mM) by the corresponding liquid volumes (mL), yielding quantities in mmol. The initial volume was 25 mL for all runs; post-deionization volumes were estimated from the average dilution factor of galactose and tagatose, ranging from 28.7 to 45.9 mL (**Table 2.4**). Galactose mass recovery across all eight runs ranged from 95.6% to 113.1%, and tagatose recovery from 89.6% to 104.8% (**Table 2.4**). Deviations from 100% are attributable to the combined measurement uncertainty of duplicate HPLC determinations and the volume estimation method. No systematic loss of either sugar was observed, and galactose and tagatose recoveries were statistically indistinguishable within each run. These results confirm that ion-exchange treatment does not selectively remove, degrade, or chemically transform monosaccharide. The apparent decrease in sugar concentration after deionization (reflected in dilution factors of 1.1-1.9, **Figure 2.3**) is therefore attributable entirely to an increase in effective liquid volume resulting from water retained in the resin matrix and pore-space displacement during batch contact. [72] These phenomena are well-established in ion-exchange processing of carbohydrate syrups and do not represent sugar loss. [73,74] The downstream evaporation step (**Section 2.2.4**) reverses this dilution by concentrating the deionized liquor to the target °Brix.

Table 2.4 Sugar mass balance. Mass = Concentration (mM) × Volume (mL) / 1000.

Run	Neutralization acid	Galactose IN (mmol)	Galactose OUT (mmol)	Gal. Rec. (%)	Tagatose IN (mmol)	Tagatose OUT (mmol)	Tag. Rec. (%)
1	CO_2	2.425	2.539	104.7	6.387	6.115	95.7
2	CO_2	2.425	2.491	102.7	6.387	6.221	97.4
3	CO_2	2.425	2.743	113.1	6.387	5.721	89.6
4	CO_2	2.425	2.319	95.6	6.387	6.702	104.8
5	H_2SO_4	1.413	1.433	101.4	9.186	9.067	98.6
6	H_2SO_4	1.413	1.434	101.5	9.186	9.059	98.6
7	H_2SO_4	1.413	1.378	97.5	9.186	9.413	102.5

Run	Neutralization acid	Galactose IN (mmol)	Galactose OUT (mmol)	Gal. Rec. (%)	Tagatose IN (mmol)	Tagatose OUT (mmol)	Tag. Rec. (%)
8	H_2SO_4	1.413	1.457	103.1	9.186	8.930	97.2

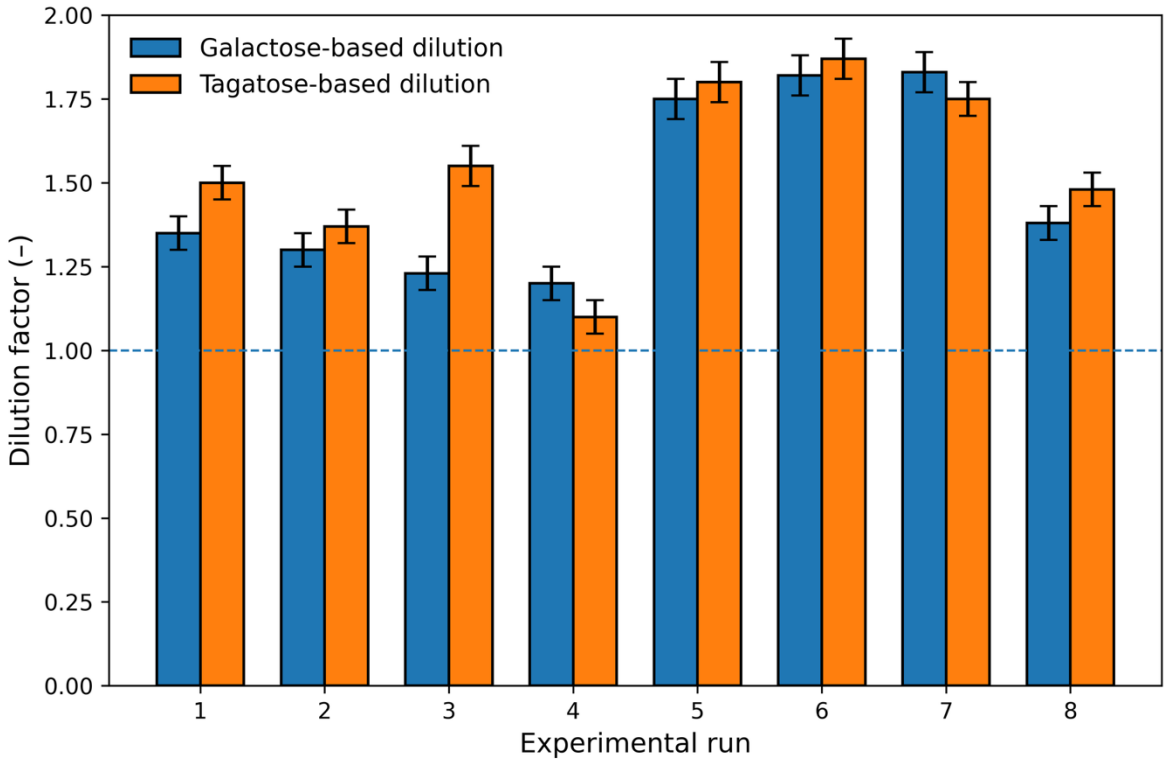

Figure 2.3 Apparent dilution factors calculated independently from galactose and tagatose concentrations measured by HPLC before and after ion-exchange deionization for experimental runs 1-8. Error bars represent the standard deviation of duplicate measurements (n = 2). The dashed line at a dilution factor of 1 indicates the hypothetical case of no dilution.

2.4 Modelling and Optimization of Resin Dosage

To quantitatively assess the influence of resin dosage and contact time on syrup deionization performance, empirical regression models were developed based on data from 19 batch ion-exchange experiments. The experimental design spanned syrup volumes of 10-300 mL, contact times of 10-30 min per exchange stage, and inlet conductivities near 2.4 mS cm^{-1}. Resin dosages were normalized by syrup volume and expressed as cation (D_c) and anion (D_a) loadings (g resin mL^{-1} syrup).

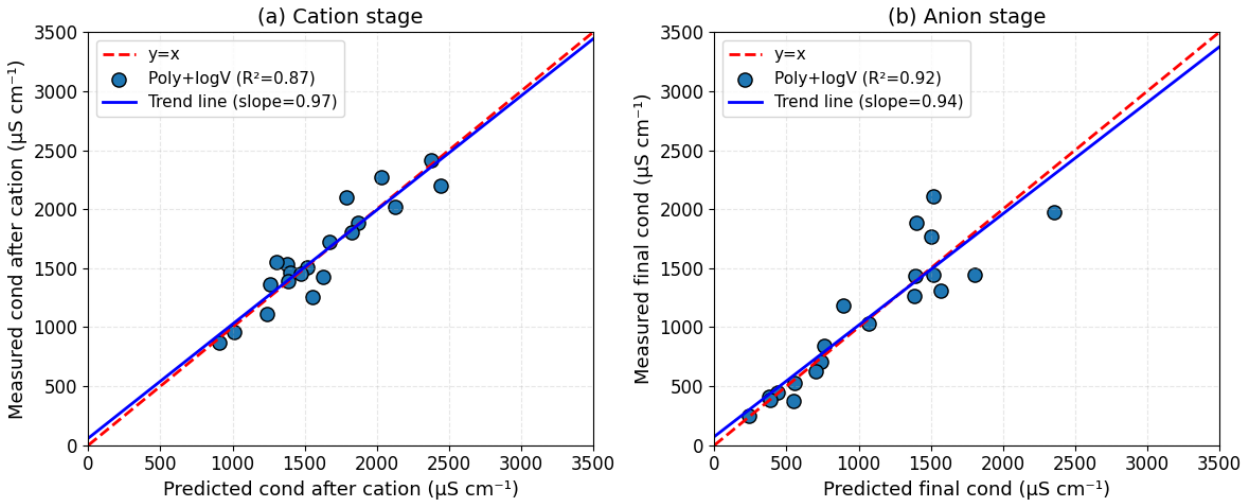

Figure 2.4 Measured versus predicted conductivity after (a) cation exchange and (b) anion exchange using second-order polynomial regression models (R^2 = 0.87 and 0.92, respectively). The trendline slopes for the cation- and anion-exchange stages were 0.97 and 0.94. The dashed lines indicate the line of parity. Regression details are provided in the Supporting Information.

2.4.1 Cation-exchange Regression

A second-order polynomial regression was used to relate the conductivity after cation exchange to the inlet conductivity, cation resin dosage, and contact time. The resulting model accurately captured the nonlinear behavior associated with ion-exchange saturation, achieving a coefficient of determination of $R^2 = 0.87$ (**Figure 2.4a**). The curvature observed in the model response indicates diminishing conductivity reduction at higher resin loadings and longer contact times, consistent with diffusion- and capacity-limited cation exchange.

2.4.1.1 Anion-exchange Regression

An analogous second-order model was developed for the anion-exchange stage using the conductivity exiting the cation step, anion resin dosage, and contact time as predictors. The anion-exchange model exhibited similarly strong predictive capability ($R^2 = 0.92$; **Figure 2.4b**) and revealed pronounced nonlinear behavior at elevated resin dosages. This response reflects saturation effects and mass-transfer limitations typical of anion exchange in concentrated sugar syrups.

2.4.1.2 Bench-scale Process Optimization

Both regression models were used to identify operating conditions that achieve substantially reduced syrup conductivity, consistent with levels commonly targeted for downstream food and bioprocessing applications. The model identified an optimal operating region characterized by moderate cation-exchange resin dosages ($D_c \approx 0.04$-0.17 g mL^{-1}), lower anion-exchange resin dosages ($D_a \approx 0.01$-0.08 g mL^{-1}), and contact times of approximately 5-30 min per exchange stage. Under these conditions, the predicted syrup conductivity approached low-conductivity values (≈ 250-300 µS cm^{-1}) while maintaining near-neutral pH. In contrast, lower resin dosages ($D_c < 0.07$ g mL^{-1} or $D_a < 0.02$ g mL^{-1}) generally resulted in incomplete deionization, with outlet conductivities frequently exceeding 500 µS cm^{-1}.

To assess the predictive capability of the polynomial regression model, a verification experiment was conducted using 300 mL of tagatose-rich syrup with an initial conductivity of 2.3 mS cm^{-1}. This condition corresponds to the upper limit of the calibration range (10-300 mL) and was used to evaluate model

performance at larger processing volumes. The optimized dosage ratios predicted by the model were scaled linearly with syrup volume, resulting in approximately 45 g of cation-exchange resin and a proportionally lower mass of anion-exchange resin, with 20 min contact time per stage. The cation resin was regenerated using 0.5 M HCl and the anion resin using 0.3 M NaOH, followed by rinsing until the rinse effluent conductivity fell below 200 μS cm^{-1}. Under these conditions, the syrup conductivity decreased from 2.3 mS cm^{-1} to 774 μS cm^{-1} after the cation-exchange step and to approximately 200 μS cm^{-1} after the anion-exchange step, following the reduction trends predicted by the model. This result demonstrates the reproducibility of the optimized ion-exchange strategy and confirms internal model consistency within the bench-scale range studied (10-300 mL). This result does not constitute process scale-up in an engineering sense but demonstrates that the empirical dosage relationships are reproducible across the volume range evaluated.

Predicted and measured values showed strong agreement across all responses (**Table 2.5**). Pearson correlation analysis indicated high correlations for the cation-exchange stage ($r = 0.93$, $p < 0.001$), anion-exchange stage ($r = 0.91$, $p < 0.001$), and pH ($r = 0.94$, $p < 0.001$). Analysis of variance confirmed that all regression models were statistically significant, with p-values of 0.036, 0.007, and 0.032 for the cation, anion, and pH models, respectively. The trendline slopes for the cation- and anion-exchange stages were 0.97 and 0.94, indicating that predicted and measured values are closely aligned, with only minimal deviation from perfect agreement.

Table 2.5 Model performance: correlation and overall significance.

Response	Pearson r	Pearson p-value	ANOVA F	ANOVA p-value
Cation conductivity	0.93	< 0.001	4.08	0.036
Anion conductivity	0.91	< 0.001	7.15	0.007
pH	0.94	< 0.001	4.26	0.032

2.4.2 Evaporation and Final Evaluation of Concentrated Tagatose-rich Syrup

Following ion-exchange deionization, the purified tagatose-rich liquor (≈7-8 °Brix) was concentrated by vacuum evaporation to produce two final high-solids syrups at 65 and 75 °Brix. These syrups represent the final product streams of the process and were subjected to physicochemical, compositional, elemental, and microbiological evaluation. Because high-solids carbohydrate syrups exhibit elevated viscosity, reduced ion

mobility, and non-ideal optical behavior, appropriate analytical handling was applied for several measurements to ensure accuracy and reproducibility.[75] The resulting data are summarized in **Table 2.6** and discussed below.

2.4.2.1 Solids Content and Analytical Handling of High-Brix Syrups

Vacuum evaporation achieved the intended concentration endpoints with high reproducibility, yielding syrups at 65.0 °Brix and 75.0 °Brix (**Table 2.6**). Measurement of soluble solids by refractometry is well suited for high-sugar matrices and was therefore performed directly on the concentrated syrups. In contrast, electrochemical measurements such as electrical conductivity are known to be unreliable when performed directly on highly concentrated carbohydrate solutions, due to increased viscosity, suppression of ion mobility, and non-linear electrode response. For this reason, conductivity measurements were carried out on 10× diluted syrup samples prior to analysis (**Table 2.6**). The use of standardized dilution for conductivity determination is a common practice in the analysis of concentrated carbohydrate syrups, including refined glucose and fructose syrups, where dilution minimizes matrix effects while preserving relative ionic composition.[76,77]

2.4.2.2 Ionic Quality After Evaporation: Conductivity, Ash, and Elemental Purity

Electrical conductivity, measured on 10× diluted samples, increased from 376 µS cm^{-1} at 65 °Brix to 455 µS cm^{-1} at 75 °Brix (**Table 2.6**). These values represent method-defined, diluted measurements and are therefore used as comparative indicators of ionic removal rather than absolute conductivity values of the native concentrated syrups. The observed increase reflects concentration-dependent changes in ionic strength and equilibria following water removal rather than deterioration of deionization performance. Total ash content remained low following evaporation and showed no increasing trend with higher °Brix, decreasing slightly from 0.13 wt% to 0.09 wt% (**Table 2.6**). In addition, elemental analysis confirmed that Pb, Cd, As, and Hg were all below the limits of detection by ICP-OES.[78] Together, these results demonstrate that vacuum evaporation did not introduce inorganic contamination and that the effectiveness of upstream deionization was preserved during concentration, consistent with the behavior reported for refined carbohydrate syrups

such as HFCS, where ion-exchange deashing followed by evaporation concentrates sugars without increasing inorganic impurities.[79,80]

2.4.2.3 Color Development and Thermal Stability During Concentration

Color development during evaporation was evaluated using A_{420} and ICUMSA color values (**Table 2.6**). Both parameters showed a gradual increase with increasing °Brix, with A_{420} rising from 0.009 at 65 °Brix to 0.011 at 75 °Brix and ICUMSA color increasing from 90 to 110 IU. This limited magnitude of color increase is consistent with mild thermal effects under vacuum conditions, where reduced boiling temperatures restrict extensive browning reactions such as caramelization and advanced Maillard chemistry.[81–83] Incremental color development with increasing solids content is well documented for refined carbohydrate syrups including glucose, fructose, and HFCS, and is generally attributed to concentration-dependent thermal effects rather than chemical degradation or impurity accumulation.[84,85] In industrial HFCS processing, similar modest increases in ICUMSA color are commonly observed during evaporation following ion-exchange purification, while maintaining low ash and metal contents.[84,86] The absence of concurrent increases in total ash or detectable metals (Pb, Cd, As, Hg) in **Table 2.6** supports this interpretation, confirming that color development arose primarily from controlled thermal concentration rather than inorganic contamination or deterioration of deionization performance.

2.4.2.4 Formation of HMF

Thermal degradation during evaporation was further assessed by quantifying HMF, a widely used indicator of heat-induced sugar degradation.[87–93] HMF concentrations remained low, below 5 mg kg^{-1} at 65 °Brix and increased slightly to 8 mg kg^{-1} at 75 °Brix (**Table 2.6**). These values are consistent with evaporation under reduced pressure and limited thermal exposure and fall within ranges reported for refined carbohydrate syrups processed under controlled conditions.[73,94] The low HMF levels align with the modest color development observed and confirm that vacuum evaporation preserved sugar integrity despite the high final solids content.

2.4.3 Water Activity and Microbiological Quality

Vacuum evaporation substantially reduced water activity, reaching 0.74 at 65 °Brix and 0.70 at 75 °Brix

(**Table 2.6**). These water activity values fall within a range widely recognized to inhibit the growth of most spoilage microorganisms in sugar-rich systems, where reduction of water activity serves as the primary preservation mechanism for concentrated liquid sweeteners, including HFCS and other refined carbohydrate syrups.[95–97] Microbiological quality of the concentrated syrups, evaluated after short-term refrigerated storage, showed low total aerobic mesophilic counts (37.5-43 CFU mL^{-1}) and moderate yeast and mold counts (225-275 CFU mL^{-1}) for the 65 and 75 °Brix samples, respectively (**Table 2.6**). No pathogenic microorganisms, including *Escherichia coli*, *Salmonella* spp., or *Staphylococcus aureus*, were detected in any sample. These results are consistent with reported microbiological profiles of concentrated tagatose-rich syrups produced via ion-exchange and evaporation, including patented formulations exhibiting similarly low bacterial counts and absence of pathogens at comparable solids contents.[98] The observed yeast and mold levels are therefore attributed to storage-related effects rather than process-induced contamination, confirming satisfactory short-term microbiological stability of the syrup.

2.4.4 Sugar Composition After Evaporation

Sugar composition analysis confirmed the chemical stability of the syrup during vacuum concentration (**Table 2.6**). Tagatose remained the dominant carbohydrate at both concentration levels, accounting for 53.5 wt% (organic dry basis) at 65 °Brix and 56.2 wt% at 75 °Brix, while galactose persisted as the primary residual impurity. Minor sugars decreased slightly with increasing °Brix.

Although the present analysis focused on the major monosaccharides, prior patent disclosures describing tagatose-rich syrups produced via alkaline epimerization and downstream purification indicate that such syrups may also contain minor non-sugar constituents. These include small amounts of oligosaccharides, glycerol, residual organic acids, and trace inorganic components originating from neutralization and ion-exchange steps, typically present at low weight fractions relative to the total carbohydrate content.[98] The stable monosaccharide composition observed here suggests that vacuum evaporation did not promote additional formation or transformation of these minor components, consistent with the compositional stability reported in the patent literature.

Table 2.6 Physicochemical, compositional, and microbiological properties of concentrated syrups.

	Unit	65 °Brix	75 °Brix	Method
Tagatose	wt% (dry basis)	53.5	56.2	HPLC-RI
Galactose (main impurity)	wt% (dry basis)	39.3	38.4	HPLC-RI
Minor sugars	wt% (dry basis)	7.2	5.4	HPLC-RI
Brix	°Brix	65.0 ± 0.2	75.0 ± 0.2	Digital refractometer
pH (25 °C)	–	7.30 ± 0.05	6.95 ± 0.05	pH meter
Water activity (a_w)	–	0.74 ± 0.01	0.70 ± 0.01	Water activity meter
Conductivity	µS/cm	376 ± 20	455 ± 20	Conductivity meter
Total ash	wt%	0.13 ± 0.02	0.09 ± 0.02	Gravimetric
Color (A_{420})	–	0.009 ± 0.001	0.011 ± 0.001	UV-Vis
ICUMSA color	IU	90 ± 10	110 ± 10	Calculated from A_{420}
Pb	ppm	< LOD	< LOD	ICP-OES
Cd	ppm	< LOD	< LOD	ICP-OES
As	ppm	< LOD	< LOD	ICP-OES
Hg	ppm	< LOD	< LOD	ICP-OES
HMF	mg kg^{-1}	4.2 ± 0.5	8 ± 2	HPLC-UV
TAMC	CFU/mL	37.5	43	Plate count
Yeast & Mold	CFU/mL	225	275	Plate count
Escherichia coli	–	N.D.	N.D.	Presence/absence
Salmonella spp.	–	N.D.	N.D.	Presence/absence
Staphylococcus aureus	–	N.D.	N.D.	Presence/absence

Notes: Values are reported as mean ± standard deviation (n = 2) for each concentration level. N.D. indicates not detected, and LOD indicates the limit of detection. Sugar composition is reported on an organic dry basis excluding ash content; therefore, values sum to 100% of the organic fraction. Microbiological results are expressed as CFU/mL due to the liquid nature of the syrup samples.

2.5 Conclusion

This study presents a process-level framework for producing tagatose-rich syrup through the integration of CaO-promoted galactose isomerization, optimized neutralization, ion-exchange deionization, and controlled vacuum evaporation. Among the neutralization routes evaluated, CO_2 neutralization demonstrated clear advantages over sulfuric acid by generating a lower ionic load and enabling more effective downstream deionization, resulting in substantially reduced residual calcium, magnesium, and sulfur-containing species. Systematic screening of strong-acid cation and strong-base anion exchange resins identified an optimal resin combination capable of reducing syrup conductivity by approximately 90%, achieving conductivity levels as low as ~250 μS cm^{-1} under the tested conditions. Empirical regression models describing the effects of resin dosage and contact time provided reasonable agreement between predicted and measured values (R^2 = 0.87-0.92) and were successfully validated at larger syrup volumes, with trendline slopes of 0.97 and 0.94 for the cation- and anion-exchange stages, respectively, indicating excellent agreement between predicted and measured conductivity values. The developed model should be considered as an empirical framework for identifying trends and guiding preliminary process design, rather than a fully predictive tool for scale-up. Following purification, vacuum evaporation to 65 and 75 °Brix produced stable, high-solids syrups with low ash content, acceptable ICUMSA color, minimal HMF formation, and preserved sugar composition, indicating that thermal concentration under reduced pressure did not compromise product quality. Microbiological evaluation after short-term refrigerated storage showed low aerobic counts, moderate yeast and mold levels, and absence of pathogens, consistent with the expected stability of concentrated carbohydrate syrups. Overall, this work demonstrates that CO_2-neutralized, ion-exchange-polished tagatose-rich syrup approaches several quality benchmarks relevant to food applications at bench scale. Mass-based ion and sugar balances confirm that conductivity reductions reflect true ionic removal, and that both sugars are conserved quantitatively. The bench-scale operating guidelines and resin selection criteria established here provide a foundation for future column-scale process development and more comprehensive process validation.

3 Chapter 3 - Functional Assessment of Tagatose-rich Syrup in Shortbread Cookie Systems

3.1 Introduction

The growing concern over excessive sugar consumption has intensified efforts to reduce added sugars in the human diet. High intake of sucrose and other refined sugars has been consistently associated with obesity, type 2 diabetes, metabolic disorders, and increased cardiovascular risk.[99–102] In response, international health organizations, including the World Health Organization (WHO), recommend limiting free sugar intake to below 10% of total daily energy, with additional benefits at even lower levels.[103] These recommendations have placed significant pressure on the food industry to reformulate products in ways that reduce sugar content while maintaining consumer acceptance.[104,105]

Among sugar-rich food categories, bakery products, particularly cookies, represent a major contributor to daily sugar intake. However, reformulating cookies is especially challenging due to the multifunctional nature of sucrose in these systems.[106] Beyond providing sweetness, sucrose plays a critical role in determining dough properties, controlling spread during baking, influencing moisture distribution, and driving color and flavor development through Maillard and caramelization reactions.[38,39] As a result, reducing or replacing sucrose often leads to undesirable changes, including reduced spread, increased hardness, lower moisture retention, and less appealing color and flavor.[47]

To address these challenges, various sugar alternatives have been explored, ranging from liquid sweeteners such as HFCS to polyols and high-intensity sweeteners.[40,106] Despite their widespread use, these options present important limitations. HFCS offers processing advantages but does not substantially improve the nutritional profile due to its similar glycemic impact.[41] Polyols can mimic bulk properties but may introduce cooling effects and digestive concerns.[42,43] High-intensity sweeteners provide sweetness without calories but lack the structural functionality required in baked products and often require complex formulation strategies to compensate for their limitations.[107] Consequently, replicating the full range of sucrose functionality in cookies remains a significant challenge.

Rare sugars have recently emerged as a promising class of alternative sweeteners with improved nutritional characteristics.[10,55,108,109] In addition to these attributes, tagatose can participate in browning reactions, suggesting that it may contribute to desirable color and flavor development in baked systems.[45,110–112] However, most existing studies have focused on highly purified tagatose, whereas practical food applications are more likely to involve syrup-based forms produced through scalable processing routes. The functional behavior of such syrups in complex food matrices remains insufficiently understood. In our previous study, a tagatose-rich syrup was produced via CaO-catalyzed galactose isomerization, followed by CO_2 neutralization and ion-exchange purification.[113] The resulting syrup contained tagatose as the major sugar component along with residual galactose and minor inorganic constituents remaining after processing. While this work demonstrated the feasibility of producing a purified tagatose-rich syrup suitable for food applications, its performance in a bakery system has not yet been evaluated. In this study, the functionality of the produced syrup was assessed in cookie formulations and compared with sucrose and HFCS in terms of spread ratio, moisture content, water activity, color (L*, a*, b*), and texture properties. This approach provides insight into the viability of tagatose syrup as an alternative to conventional sugars.

3.2 Methods and Materials

Pastry flour and unsalted butter were obtained from local suppliers. Granulated sucrose (Great Value®, Walmart, USA) was used as the crystalline sweetener control. Commercial HFCS-42 (Golden Barrel, USA) was used as a liquid sweetener. The syrup contained approximately 70-71.8% solids, and the dry solids fraction consisted of approximately 42% fructose. The syrup was concentrated to 80 °Brix using rotary evaporation to match the solids content of the experimental tagatose syrup. Tagatose-rich syrup (80 °Brix) used in this study was produced according to the optimized process described in our previous work and briefly summarized below.

3.2.1 Preparation of Tagatose-rich Syrup

Tagatose-rich syrup used in this study was prepared based on the optimized method developed in our previous work.[113] Briefly, galactose was subjected to CaO-promoted alkaline isomerization under ambient conditions,

followed by neutralization using CO_2 to precipitate calcium as $CaCO_3$. The resulting slurry was clarified by filtration to remove solid precipitates. The clarified syrup (approximately 7 °Brix) was subsequently purified via sequential cation (DIAION PK212) and anion (DIAION PA312) ion-exchange treatment to remove residual inorganic ions. Under optimized conditions, conductivity was reduced to ≤250 μS cm^{-1} (measured on diluted samples), indicating effective deionization. The purified syrup was then concentrated using rotary vacuum evaporation at 50 °C to a final solids content of 80 °Brix. Sugar composition was quantified using an Agilent 1200 HPLC system equipped with a refractive index (RI) detector and a Rezex RPM-Monosaccharide column (Phenomenex, USA), following the analytical procedure described in our previous study. Deionized water was used as the mobile phase at a flow rate of 0.6 mL min^{-1}, and the column temperature was maintained at 80 °C. Quantification of tagatose and galactose was performed using external calibration curves prepared from analytical standards. HMF was quantified using an Agilent Technologies 1260 Infinity HPLC system equipped with a UV detector and a Bio-Rad Aminex HPX-87H ion-exclusion column (300 × 7.8 mm). The column temperature was maintained at 65 °C, and 5 mM H_2SO_4 was used as the mobile phase at a flow rate of 0.6 mL min^{-1}. The resulting syrup contained approximately 57.8 wt% tagatose and 34.3 wt% galactose (organic dry basis) and was used directly in cookie formulation.

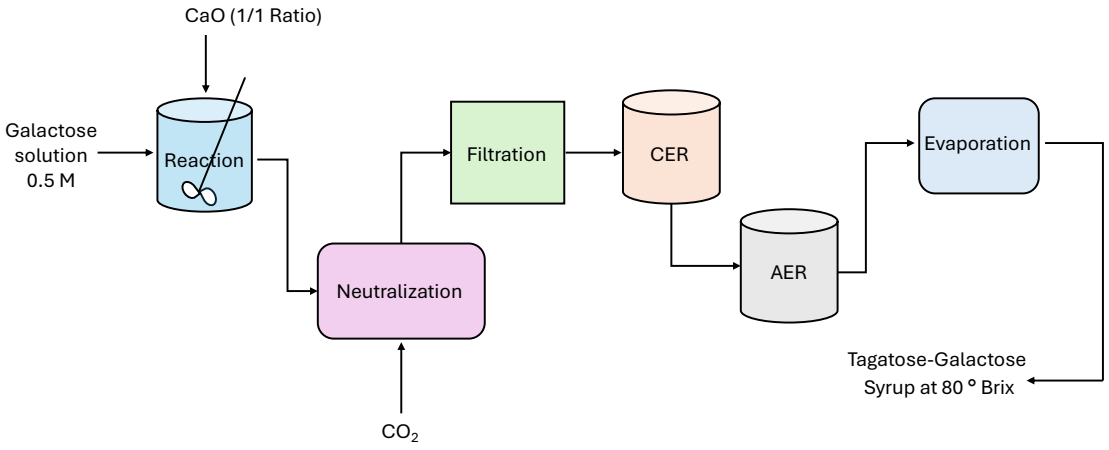

Figure 3.1 Schematic representation of the tagatose-rich syrup production and purification process adapted from our previous work and used for preparation of the experimental syrup evaluated in this study.[113]

3.2.2 Cookie and Cookie Dough Formulation and Preparation

Shortbread cookie formulation was used in this study (**Table 3.1**). Three formulations were prepared by replacing sucrose with either 80 °Brix HFCS or 80 °Brix tagatose-rich syrup at 100% substitution (dry basis). To ensure equivalent solids content across all treatments, additional water was added to the sucrose formulation to match the moisture content of the syrup-based systems. Doughs for baked cookies and dough texture analysis were prepared separately following the same mixing procedure. Butter and sweetener were creamed using a stand mixer (KitchenAid) at speed 4 for 8 min, with scraping at 2- and 4-min intervals. Flour was gradually incorporated and mixed until fully combined, followed by mixing at speed 2 for 1 min.

For dough texture analysis, the dough was divided and shaped into cylindrical samples with a diameter of 2.54 cm and a height of 1.30 cm, and six samples were analyzed per batch using a texture analyzer. For baked cookie evaluation, the dough was portioned into 100 g samples, rolled into cylindrical logs (approximately 5.08 cm diameter), chilled for 10 min, and sliced into 1.30 cm thick pieces prior to baking. Cookies were baked in a reel rotating oven at 177 °C for 20 min on aluminum sheet pans lined with parchment paper.

A total of nine batches were prepared for each dough type, consisting of three batches per different sugar formulations (sucrose, HFCS, and tagatose). For baked cookies, 20 cookies were produced per batch, whereas for dough analysis, six samples per batch were tested.

Table 3.1 Shortbread cookie formulation (% flour basis) and corresponding batch sizes (g) for dough samples used in texture analysis and for baked cookie production.

Ingredients	% flour basis	Original formulation (g)
Unsalted Butter	75.0	112.5
Sucrose, HFCS, Tagatose	33.3	50.0
Pastry Flour	100.0	150.0
Salt	1.0	1.4

Values are reported on a dry basis for sweeteners.

3.2.3 Physical Properties of Cookies

Cookie diameter was measured using a digital caliper by averaging measurements taken from two directions

for each cookie. Thickness was determined by stacking six cookies and measuring the total height, which was then divided by six to obtain average thickness per cookie. The spread ratio was calculated as:

$$\text{Spread Ratio} = \frac{\text{Diameter}}{\text{Thickness}} \quad (1)$$

3.2.4 Color Measurement and BI

Color measurements (L*, a*, b*) were performed using a Konica Minolta BC-10 Plus baking meter/colorimeter (Konica Minolta, Japan). For each batch, three cookies were selected and three different locations on each cookie surface were measured, resulting in nine measurements per batch. Mean values were calculated and used for analysis. Total color difference (ΔE) was calculated relative to the sucrose control using the CIELAB equation:[114]

$$\Delta E = \sqrt{(L - L_0)^2 + (a - a_0)^2 + (b - b_0)^2} \quad (2)$$

where L_0, a_0, and b_0 correspond to the mean color values of the first sucrose batch.

In addition, the BI was calculated to quantify the extent of browning based on CIELAB parameters.[48] The intermediate variable x was first determined as:

$$x = \frac{a^* + 1.75L^*}{5.645L^* + a^* - 3.012b^*} \quad (3)$$

and the BI was then calculated as:

$$\text{BI} = \frac{100(x - 0.31)}{0.17} \quad (4)$$

3.2.5 Texture Analysis

Texture properties of cookie dough and baked cookies were evaluated using a texture analyzer (Stable Micro Systems TA-XT plus, UK) equipped with a 5 kg load cell. Cookie dough was analyzed in compression mode using a 25 mm acrylic cylindrical probe with radiused edges (P/36R, AACC method) at pre-test, test, and post-test speeds of 1.0, 1.7, and 10.0 mm/s, respectively, with a target strain of 35%, an auto-trigger force of 5 g, and a data acquisition rate of 250 pps. Firmness was determined as the maximum compression force, and adhesiveness was obtained from the negative force recorded upon probe retraction. Baked cookies were analyzed using a 3-point bend rig (TA-092NS). Pre-test, test, and post-test speeds were 1.0, 3.0, and 10.0 mm/s, respectively, with a travel distance of 5 mm, an auto-trigger force of 50 g, and a data acquisition rate

of 500 pps. Each cookie was placed centrally on the support and force was applied at the midpoint until fracture occurred. Hardness was defined as the maximum force required to break the sample, and fracturability was defined as the distance at fracture, representing the flexibility of the cookie. Six measurements were conducted for each batch, and average values were reported.

3.2.6 Moisture Content and Water Activity

Moisture content of baked cookies was determined using a moisture analyzer (Mettler Toledo HE73). Water activity (a_w) was measured using a water activity meter (AquaLab 4TE, METER Group) at ambient temperature.

3.2.7 Experimental Design and Statistical Analysis

All experiments were conducted using three independent batches for each treatment (sucrose, HFCS, and tagatose syrup). Approximately 20 cookies were prepared per batch, and subsets of samples were used for each analytical measurement. Data were analyzed using one-way ANOVA followed by Tukey's honestly significant difference (HSD) post-hoc test (Microsoft Excel Data Analysis ToolPak). Differences were considered statistically significant at $p < 0.05$.

3.3 Results and Discussion

3.3.1 Physicochemical Characterization of Sugar Syrups

The physicochemical properties of the tagatose syrup produced in this study were evaluated and compared with those of commercial HFCS to ensure that differences observed in cookie performance were attributable to sugar type rather than variations in syrup quality.

3.3.1.1 Sugar Composition

HPLC analysis confirmed that the produced syrup consisted primarily of tagatose (≈57.8 wt%) and galactose (≈34.3 wt%) on an organic dry basis, with minor amounts of by-products. This composition is consistent with the results reported in our previous study, confirming reproducibility of the isomerization and purification process at the 500 ml scale. In contrast, HFCS-42 consisted predominantly of fructose (~42%) and glucose, representing a typical composition of commercial liquid sweeteners.[73] The presence of reducing sugars in

both HFCS and tagatose syrup suggests potential participation in Maillard reactions during baking, although differences in sugar reactivity are expected to influence browning behavior.[115,116]

3.3.1.2 Implications for Cookie Applications

The produced tagatose syrup showed low mineral content, low color, and minimal thermal degradation (**Table 3.2**). These compositional characteristics are adequate for the purposes of this study, where the syrup is evaluated as a research material to investigate its functional role in cookie systems rather than as a finished or food grade product. Any differences observed in cookie properties can therefore be attributed primarily to intrinsic differences in sugar chemistry rather than to impurities or artifacts from syrup preparation.

Although galactose represents a substantial fraction (~34 wt%) of the produced syrup, its functional impact in the cookie system is expected to be reinforcing rather than disruptive. Galactose shares several key physicochemical features with tagatose: both are monosaccharides of similar molecular weight, both are reducing sugars that participate in Maillard reactions, and both exhibit comparable water-binding behavior. As a result, the syrup functions as a unified low-glycemic, reducing-sugar sweetener system rather than a binary mixture with conflicting properties. The most likely contribution of residual galactose is to reinforce the Maillard reactivity and water-retention behavior of tagatose, rather than dilute its functionality. The specific implications of this combined sugar profile on dough rheology, browning, and cookie texture are examined in the following sections.

Table 3.2 Physicochemical composition and properties of sweeteners used in cookie formulations

Parameter	Tagatose-rich Syrup	HFCS	Sucrose
Tagatose, wt% organic dry basis	57.8	–	–
Galactose, wt% organic dry basis	34.3	–	–
Minor Sugars/by-products, wt% organic dry basis	7.9	–	–
Fructose, wt% organic dry basis	–	42	–

Parameter	Tagatose-rich Syrup	HFCS	Sucrose
Glucose and other saccharides, wt% dry basis	–	58	–
Ash, wt%	0.24	0.05	N.D.
HMF (mg kg^{-1})	5.12	7.43	N.D.
pH	5.1	6.34	–
A_{420}	0.014	0.025	–

Note: Dashes indicate parameters not applicable to crystalline sucrose or not measured. N.D. indicates not detected.

3.3.2 Textural Properties of Cookie Dough

The texture behavior of cookie dough formulated with sucrose, HFCS, and tagatose syrup was evaluated through force-time profiles (**Figure 3.2**) and quantitative parameters (**Table 3.2**). Clear differences were observed in both the deformation behavior and stickiness of the dough systems, reflecting the distinct physicochemical properties of the sweeteners. From the force-time curves (**Figure 3.2**), all samples exhibited a gradual increase in force until reaching a maximum, followed by a sharp drop corresponding to structural breakdown. However, while the magnitude and shape of these curves varied among the formulations, no statistically significant differences in hardness were detected ($p > 0.05$). The tagatose dough showed the highest peak force (~704.70 g), followed by sucrose (~661.01 g) and HFCS (~595.11 g) (**Table 3.2**). Indicating that tagatose dough was the firmest, with a hardness approximately 6.6% higher than sucrose and ~18.4% higher than HFCS. The differences in dough firmness can be partly explained by the aqueous solubility of each sweetener. Tagatose has a markedly lower water solubility (~58 g/100 mL at 20°C) compared to sucrose (~200 g/100 mL), while HFCS, being an aqueous syrup, is already fully dissolved and immediately available to plasticize the dough matrix. Lower solubility means less tagatose dissolves in the aqueous phase of the dough, resulting in reduced plasticization, increased resistance to deformation, and lower adhesiveness. Conversely, the high effective concentration of dissolved sugars in HFCS maximizes water binding and intermolecular disruption of the gluten-starch network, directly contributing to its softer

structure.[117] Unlike HFCS, which is a fully liquid and highly hygroscopic system rich in fructose and glucose, tagatose syrup contains less hygroscopic sugars and exhibits different water-binding behavior, , resulting in reduced molecular mobility within the dough matrix and stronger resistance to deformation.[118] This results in reduced molecular mobility within the dough matrix and a stronger resistance to deformation. In contrast, HFCS promotes softening due to its ability to disrupt intermolecular interactions within the gluten-starch network, leading to a ~10% reduction in hardness compared to sucrose.[38,40] The sucrose dough showed intermediate behavior, consistent with its crystalline nature, which limits immediate dissolution and reduces its plasticizing capacity.[38,118] The differences are also evident in the deformation profiles. The tagatose curve shows a steeper drop after the peak force, indicating a more brittle-like structural failure, whereas HFCS exhibits a more gradual decline, suggesting a more ductile and deformable matrix. Sucrose again displays intermediate behavior. These observations confirm that HFCS enhances ductility, while tagatose promotes a more rigid and less deformable structure. Adhesiveness values further highlight the differences in dough behavior. HFCS exhibited the highest magnitude of adhesiveness (-75.74 g·s), followed closely by tagatose (-71.06 g·s), while sucrose showed a significantly lower value (-41.56 g·s) (**Table 3.2**). This corresponds to an increase of approximately 82% (HFCS) and 71% (tagatose), respectively. Although these differences were not statistically significant ($p = 0.081$), a consistent trend toward higher stickiness in HFCS- and tagatose-based doughs was observed. The higher adhesiveness of HFCS is directly related to its high fructose content, which strongly binds water and creates a viscous, tacky matrix. Tagatose also shows high adhesiveness, which may be attributed to its humectant properties and the presence of residual sugars such as galactose, contributing to increased surface interactions. The negative force region in the force-time curves (**Figure 3.2**) further supports this observation, where both HFCS and tagatose exhibit larger negative areas compared to sucrose, confirming greater stickiness. Notably, tagatose shows a sharp negative peak, suggesting strong adhesive interactions during probe withdrawal, while HFCS exhibits a broader negative region, indicating sustained stickiness over time.

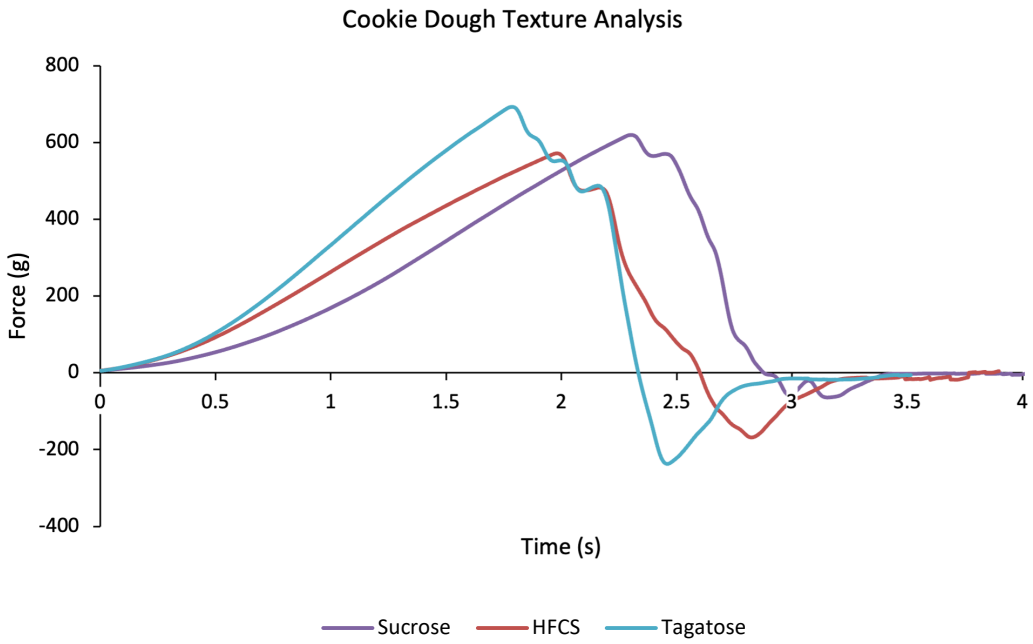

Figure 3.2 Cookie dough texture profiles for dough mad with three different formulations using Sucrose, HFCS, and Tagatose syrup.

Table 3.3 Textural properties (Firmness and adhesiveness) of cookie dough formulations prepared with sucrose, HFCS, and tagatose syrup (mean ± standard deviation).

Sample	Firmness (g)	Adhesiveness (g·s)
Sucrose	661.01 ± 144.02	-41.56 ± 20.32
HFCS	595.11 ± 44.03	-75.74 ± 16.87
Tagatose	704.70 ± 126.73	-71.06 ± 15.66

3.3.3 Color Development of Cookies

The color attributes of baked cookies were significantly affected by the type of sugar used (**Figure 3.3a & Figure 3.3b**). Lightness (L*) differed significantly among the formulations ($p < 0.01$). Cookies prepared with tagatose syrup exhibited the lowest L* values (~55.43)^{b}, while sucrose (~65.14)^{a} and HFCS (~62.42)^{a} were not significantly different from each other, indicating substantially darker surfaces. In contrast, sucrose-based cookies showed the highest lightness values, corresponding to a lighter appearance with minimal browning. The redness parameter (a*) was strongly influenced by sugar type ($p < 0.001$). Tagatose cookies exhibited the highest a* values (~15.78)^{c}, followed by HFCS (~9.69)^{b}, while sucrose showed the lowest values (~5.36)^{a}, with all three treatments significantly different from each other. This corresponds to an increase of approximately 190% for tagatose and ~80% for HFCS relative to sucrose, indicating a pronounced

enhancement in browning intensity. The significantly higher a* values observed in tagatose formulations are attributed to its strong reducing nature, which accelerates Maillard reactions during baking.[115] Unlike sucrose, which is non-reducing and must first undergo hydrolysis, tagatose readily reacts with amino groups in the dough matrix, promoting rapid formation of brown-colored compounds.[38,116,119] HFCS also participates in Maillard reactions due to its glucose and fructose content; however, its effect was less pronounced than tagatose under identical conditions.[39,40,120] An additional contributor to the enhanced Maillard browning of cookies made with tagatose syrup is the presence of galactose, which constitutes approximately 34 wt% of the produced syrup. Galactose is itself a highly reactive reducing sugar that undergoes Maillard reactions at rates comparable to glucose under baking conditions.[121] The strong browning response observed in these cookies therefore likely reflects the combined Maillard reactivity of both tagatose and galactose, rather than tagatose alone.

Similarly, the yellowness parameter (b*) was significantly affected by sugar type ($p < 0.001$). Tagatose cookies exhibited the highest b* values (~37.23)^{c}, followed by HFCS (~32.36)^{b}, while sucrose showed the lowest values (~25.53)^{a}, with all three significantly different from each other. This represents an increase of approximately 46% for tagatose and 27% for HFCS relative to sucrose. To further quantify browning development, the BI was calculated based on CIELAB parameters (**Figure 3.3b**). BI values differed significantly among treatments ($p < 0.001$), confirming the trends observed in L*, a*, and b*. Tagatose cookies exhibited the highest BI (~124.4)^{c}, followed by HFCS (~82.5)^{b}, while sucrose showed the lowest values (~54.6)^{a}, with all three treatments significantly different from each other. This represents an increase of approximately 128% for tagatose and ~51% for HFCS relative to sucrose. The substantially higher BI observed for tagatose further confirms its strong participation in Maillard reactions, resulting in intensified browning compared to both sucrose and HFCS. The ΔE was also significantly affected by sugar type ($p < 0.001$). Sucrose-based cookies exhibited the lowest ΔE values (~3.10), as expected given that sucrose served as the color reference. HFCS cookies showed intermediate deviation (~8.87), while tagatose cookies exhibited the highest ΔE (~18.55), indicating the greatest overall color departure from the sucrose standard. All three

treatments differed significantly from each other (Tukey's HSD, $p < 0.05$). ΔE values were calculated relative to the mean color values averaged across all three sucrose batches ($L_0 = 65.14$, $a_0 = 5.36$, $b_0 = 25.53$), and individual values were obtained from nine measurements per treatment (three measurements per cookie across three cookies), followed by averaging. The higher ΔE observed for tagatose is consistent with its substantially lower L* and higher a* and b* values, confirming the extent of Maillard browning in tagatose-based formulations. Individual values were obtained from nine measurements per treatment (three measurements per cookie across three cookies), followed by averaging. The lower ΔE observed for tagatose suggests a more consistent browning pattern, while sucrose exhibited greater variability in color formation. The visual appearance of the cookies (**Figure 3.4**) further confirms the instrumental color measurements, with tagatose cookies exhibiting noticeably darker surfaces compared to sucrose and HFCS samples.

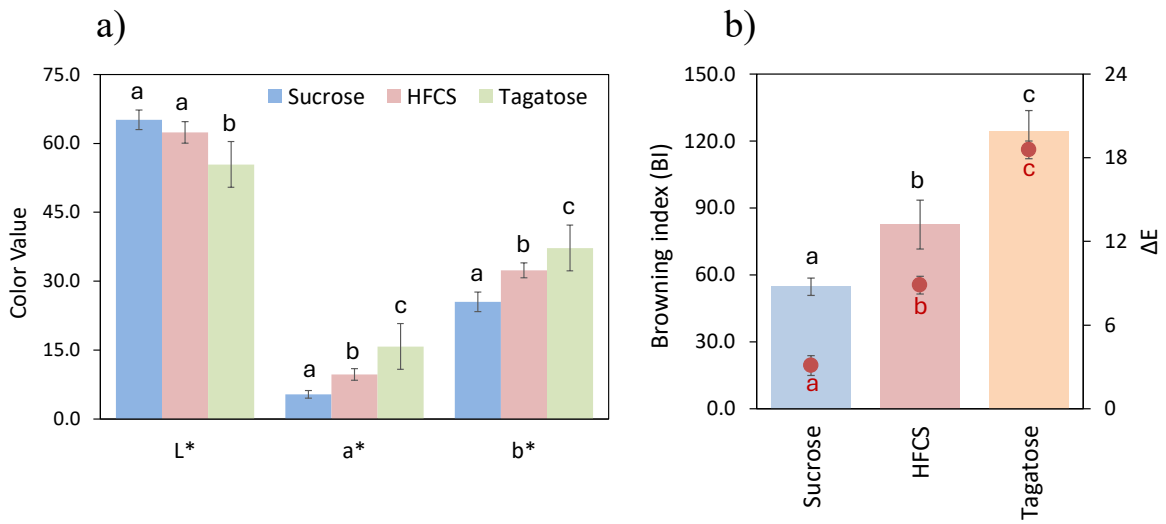

Figure 3.3 Color and browning characteristics of cookies prepared with sucrose, HFCS, and tagatose syrup. (a) CIELAB color parameters (L*, a*, b*) measured on the cookie surface. (b) BI (left axis, bars) and total color difference (ΔE; right axis, markers) of the same formulations. ΔE values were calculated relative to the mean color averaged across all sucrose batches. Bars and markers represent mean values, and error bars indicate standard deviation (n = 3). Different sugar systems significantly affected all measured parameters ($p < 0.001$). Different letters above bars indicate statistically significant differences among treatments (Tukey's HSD, $p < 0.05$).

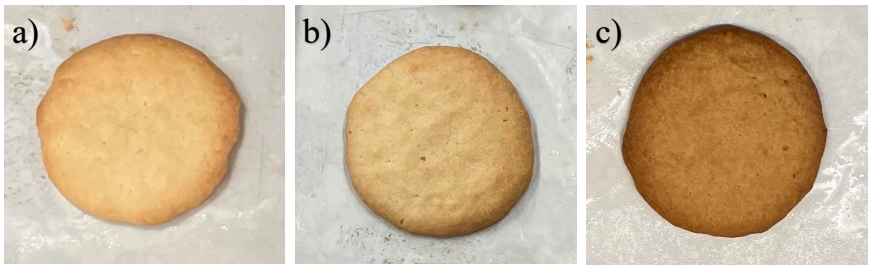

Figure 3.4 Visual appearance of cookies prepared with (a) sucrose, (b) HFCS, and (c) tagatose syrup under identical baking conditions. Tagatose cookies exhibited darker surfaces consistent with lower L* and higher a* and b* values.

3.3.4 Spread, Diameter, and Thickness of Baked Cookies

The geometrical properties of baked cookies, including spread ratio, diameter, and thickness, were significantly influenced by the type of sugar used (**Figure 3.5**). These differences reflect variations in dough viscosity, water mobility, and the timing of structure setting during baking. These differences reflect variations in dough viscosity, water mobility, and the timing of structure setting during baking. The spread ratio showed a clear dependence on sugar type, with HFCS cookies exhibiting the highest values (≈5.5^{a}), followed by sucrose (≈5.1^{b}), while tagatose resulted in the lowest spread (≈4.6^{c}). This corresponds to an increase of approximately 8% for HFCS and a decrease of about 10% for tagatose relative to sucrose. The enhanced spreading behavior of HFCS can be attributed to its liquid nature and high content of low-molecular-weight sugars, which increase dough fluidity and promote lateral flow before structure stabilization.[38,118] In contrast, tagatose-containing doughs exhibited restricted spread and reduced lateral flow during baking. This behavior is likely driven by the lower water solubility of tagatose (~58 g/100 mL at 20°C) compared to sucrose (~200 g/100 mL), which limits dissolution in the aqueous dough phase and reduces plasticization of the gluten-starch matrix. The reduced plasticization promotes earlier viscosity development and structure setting during the temperature ramp of baking. Furthermore, the lower hygroscopicity of tagatose restricts water redistribution within the dough, further limiting lateral flow before structural stabilization occurs.[117] These trends were further supported by diameter measurements, which were significantly affected by sugar type ($p < 0.001$). HFCS cookies exhibited the largest diameter (6.62 cm^{a}), followed by tagatose (6.34 cm^{b}) and sucrose (6.13

cm[c]), corresponding to increases of approximately 8% and 3%, respectively, relative to sucrose. The larger diameter of HFCS cookies is consistent with increased dough mobility and delayed structure setting, allowing greater expansion during baking.[38] Although tagatose cookies exhibited limited spread, their diameter remained slightly higher than sucrose, suggesting that factors such as gas retention and structural rigidity also contribute to final cookie dimensions. In contrast, thickness exhibited an inverse relationship with spread and was also significantly affected by sugar type ($p < 0.001$). Tagatose cookies showed the greatest thickness (≈1.38 cm[a]), followed by sucrose (≈1.20 cm[b]) and HFCS (≈1.20 cm[b], slightly lower), representing an increase of approximately 15% for tagatose compared to sucrose. The higher thickness of tagatose cookies is consistent with reduced lateral flow and indicates earlier structure formation during baking, which limits collapse and promotes vertical development.[122] Conversely, HFCS cookies exhibited lower thickness due to prolonged spreading before structure stabilization, resulting in a wider but thinner geometry.

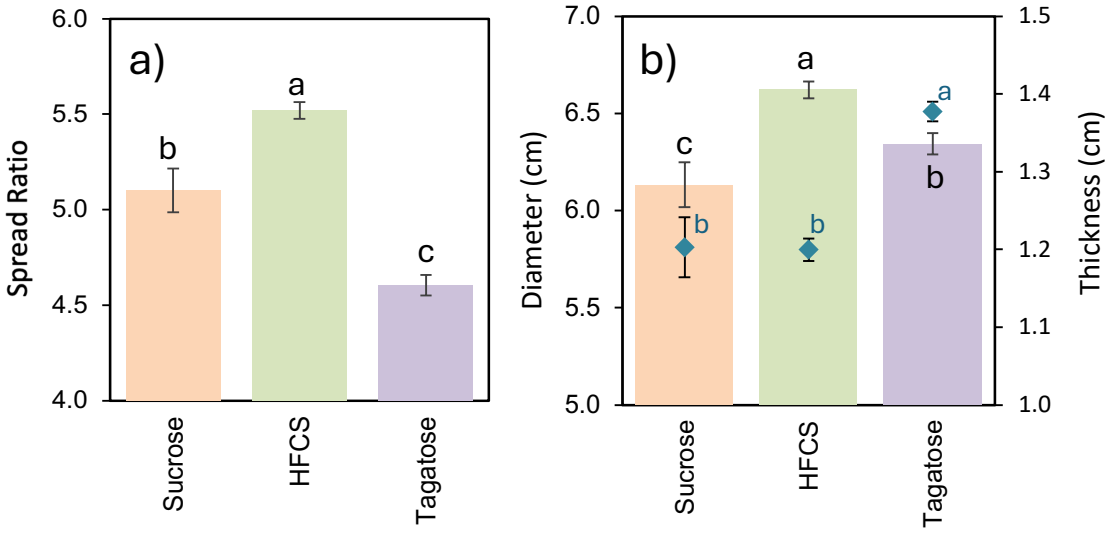

Figure 3.5 Spread ratio (a), and diameter (bars, left axis) and thickness (blue diamonds, right axis) (b) of cookies prepared with sucrose, HFCS, and tagatose syrup. Data are expressed as mean ± standard deviation (n = 3).

3.3.5 Texture Properties of Baked Cookies

The hardness of baked cookies was significantly influenced by the type of sugar used ($p < 0.01$), as shown in **Figure 3.6**. Sucrose-based cookies exhibited the highest hardness (930.83 g[a]), while tagatose (354.70 g[b]) and

HFCS (260.61 g^b) formulations showed substantially lower values, corresponding to reductions of approximately 62% and 72%, respectively, relative to sucrose. Both HFCS and tagatose were significantly softer than sucrose but did not differ significantly from each other, indicating that replacing sucrose with either sweetener results in a comparably softer cookie structure. The superior hardness of sucrose cookies is largely attributed to its high glass transition temperature (Tg ≈ 65°C), which places the baked product well below Tg at room temperature, promoting a rigid, glassy structure through crystallization during cooling.[118] In contrast, HFCS has a substantially lower Tg due to its high fructose content (Tg of fructose ≈ 5°C), meaning HFCS-based cookies exist in a rubbery, plasticized state at room temperature, which significantly weakens structural integrity through increased moisture retention and matrix softening. [40,43] Tagatose, with a Tg of approximately 17-20°C in its amorphous form, also remains near or above the glass transition at ambient conditions, producing a similarly soft structure with limited crystallization and reduced rigidity compared to sucrose. In contrast to hardness, fracturability was not significantly affected by sugar type ($p = 0.869$). The measured values were relatively close across all treatments, with tagatose (0.763 mm) and sucrose (0.758 mm) showing slightly higher deformation at break compared to HFCS (0.705 mm). This suggests that while sugar type strongly influences the force required to break the cookies, it does not significantly alter the deformation behavior at the fracture point; the internal structure differs in strength, but the failure mechanism remains similar across all formulations.

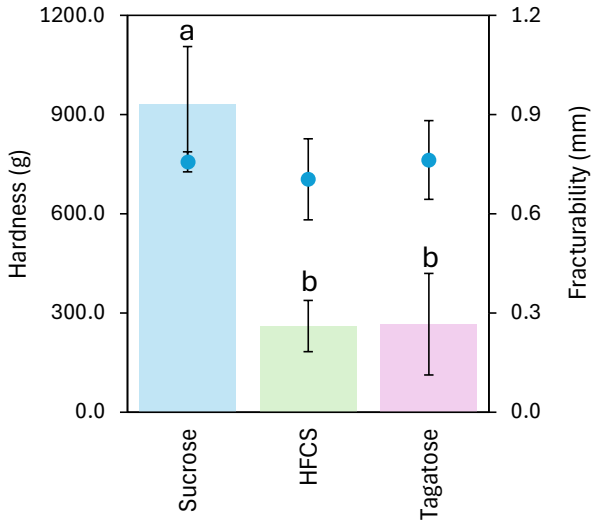

Figure 3.6 Hardness (bars, left axis) and fracturability (blue circles, right axis) of cookies prepared with sucrose, HFCS, and tagatose syrup. Values are reported as mean ± standard deviation (n = 3). Different sugar systems significantly affected hardness ($p < 0.01$), while no significant differences were observed in fracturability ($p > 0.05$).

3.3.6 Moisture Content and Water Activity

The moisture content of the cookies was significantly affected by the type of sugar used ($p < 0.01$), as shown in **Figure 3.7**. Cookies prepared with tagatose exhibited the highest moisture content (4.63%)^{a}, followed by HFCS (4.04%)^{ab} and sucrose (3.36%)^{b}. Tagatose retained significantly more moisture than sucrose, an increase of approximately 38%. HFCS showed an intermediate numerical value, approximately 20% higher than sucrose, but this difference did not reach statistical significance. The higher moisture retention observed in the tagatose system can be attributed to its hygroscopic nature, which promotes water binding and reduces moisture loss during baking. [117,123] In contrast, sucrose, owing to its crystalline behavior and lower affinity for water, produced a drier final structure. Water activity, however, was not significantly affected by sugar type ($p > 0.05$), although numerical differences were observed (HFCS: 0.478; tagatose: 0.408; sucrose: 0.382). While these trends did not reach statistical significance, they may suggest that tagatose binds a greater fraction of its retained water within the matrix rather than as free water,[124] a hypothesis that would warrant confirmation with a larger sample size. From a structural perspective, the significantly higher moisture content of tagatose cookies, combined with their balanced mechanical behavior observed in texture analysis, is

consistent with a matrix in which water is retained but partially immobilized. Sucrose cookies, with the lowest moisture content and a more crystalline structure, supported the formation of a firmer and more rigid matrix.

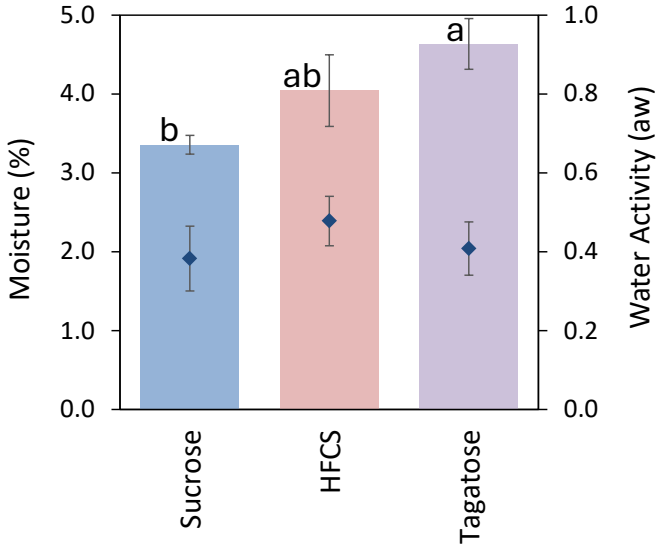

Figure 3.7 Moisture content (bars, left axis) and water activity (diamond markers, right axis) of cookies prepared with sucrose, HFCS, and tagatose syrup. Values are presented as mean ± standard deviation (n = 3). Moisture content was significantly affected by sugar type ($p < 0.01$), while no significant differences were observed in water activity ($p > 0.05$). Different letters above bars indicate statistically significant differences among treatments (Tukey's HSD, $p < 0.05$).

3.4 Conclusion

This study demonstrated that tagatose-rich syrup produced via CaO-catalyzed isomerization and downstream purification can be effectively applied in cookie formulations as a functional alternative to conventional sugars. The results highlight the critical role of sugar type in determining both dough behavior and final product quality. Tagatose syrup significantly enhanced Maillard browning, as confirmed by both CIELAB parameters and BI, resulting in darker and more uniformly developed cookie color. At the same time, it influenced structural development during baking, leading to reduced spread and increased thickness. In terms of texture, tagatose produced cookies that were substantially softer than sucrose-based samples while maintaining greater structural integrity than HFCS systems. Its ability to retain moisture while limiting water

activity further contributed to balanced textural properties. This work extends beyond conventional ingredient substitution studies by directly linking upstream syrup production to downstream food application. This integrated approach provides a more realistic framework for evaluating the feasibility of rare sugars in practical food systems. Future work should focus on process optimization, scale-up, and sensory evaluation to further support industrial implementations.

4 Chapter 4 - Conclusions and Future Directions

4.1 Conclusions

This thesis addressed key challenges in the production and application of tagatose-rich syrups by integrating upstream reaction chemistry, downstream purification, and functional food evaluation into a single framework. The results from Chapter 2 demonstrate that neutralization strategy plays a critical role in determining the efficiency of downstream purification. The choice between CO_2 and H_2SO_4 does not simply terminate the isomerization reaction; it defines the ionic composition of the resulting syrup and directly influences ion-exchange performance. CO_2-neutralized systems consistently exhibited lower initial conductivity and enabled more effective removal of residual ions, whereas H_2SO_4-neutralized systems introduced sulfate species that limited deionization efficiency. Sequential cation-anion exchange proved to be an effective approach for reducing conductivity and divalent ion content, supporting the production of syrups that meet high quality requirements. The empirical models developed in this work further provide a practical tool for predicting conductivity reduction as a function of resin dosage and contact time, offering guidance for process optimization at the bench scale. Chapter 3 extends these findings by evaluating how the purified tagatose-rich syrup performs in a real food system. The results show that replacing sucrose or HFCS with tagatose syrup leads to distinct changes in dough and baked product properties. Increased Maillard browning, differences in moisture behavior, and variations in texture highlight the dual role of tagatose as both a sweetener and a reactive component in food matrices. The observed differences in hardness and adhesiveness confirm that formulation behavior cannot be predicted solely from compositional similarity to traditional sugars. These findings emphasize that successful implementation of alternative sweeteners requires consideration of both chemical reactivity and structural effects in the final product. Taken together, this work establishes a clear connection between reaction conditions, purification strategy, and end-use functionality. It demonstrates that efficient production of tagatose-rich syrups is not solely a question of yield, but also of controlling impurities, process conditions, and their downstream implications. The integration of these aspects provides a more comprehensive basis for advancing tagatose as a viable ingredient in food systems.

4.2 Future Directions

While this study provides a strong foundation for the production and application of tagatose-rich syrups, several areas require further investigation to support scale-up and broader industrial adoption. From a process perspective, future work should focus on scaling the ion-exchange purification system from batch to continuous operation. Continuous fixed-bed or simulated moving bed systems could significantly improve process efficiency, reduce resin consumption, and provide more stable product quality. In addition, a more detailed understanding of resin fouling, regeneration efficiency, and long-term performance is necessary to evaluate operational sustainability. The influence of neutralization chemistry also warrants deeper investigation. Quantitative speciation of ionic species formed during CO_2 and acid neutralization would provide greater insight into their interactions with ion-exchange resins. Coupling experimental work with thermodynamic or transport modeling could further clarify the mechanisms governing ion removal and support process design at larger scales. From a product development perspective, additional studies are needed to evaluate the performance of tagatose-rich syrups across a wider range of food systems. While this work focused on shortbread cookies, applications in beverages, dairy products, and other baked goods may present different challenges related to solubility, stability, and sensory perception. Sensory evaluation and consumer acceptance studies will be particularly important for translating functional performance into market viability. Further research should also explore strategies to control Maillard browning and reactivity of tagatose in thermal processing. While enhanced browning can be desirable in some applications, excessive color formation or off-flavor development may limit its use. Approaches such as formulation adjustments, process condition optimization, or partial substitution strategies could help balance these effects. Finally, a techno-economic analysis and life cycle assessment is needed to fully evaluate the sustainability of tagatose-rich syrup production. This should include detailed analysis of energy consumption, raw material sourcing, resin usage, and waste streams. Integrating economic and environmental metrics will be essential for positioning tagatose as a competitive alternative to conventional sweeteners.

4.3 References

1 P. J. Rogers, The role of low-calorie sweeteners in the prevention and management of overweight and obesity: evidence v. conjecture, *Proc. Nutr. Soc.*, 2018, **77**, 230–238.

2 Reducing free sugars intake in adults to reduce the risk of noncommunicable diseases, https://www.who.int/tools/elena/interventions/free-sugars-adults-ncds, (accessed 23 April 2026).

3 S. Amarya, K. Singh and M. Sabharwal, Health consequences of obesity in the elderly, *Journal of Clinical Gerontology and Geriatrics*, 2014, **5**, 63–67.

4 L. Poston, R. Caleyachetty, S. Cnattingius, C. Corvalán, R. Uauy, S. Herring and M. W. Gillman, Preconceptional and maternal obesity: epidemiology and health consequences, *Lancet Diabetes Endocrinol.*, 2016, **4**, 1025–1036.

5 D. Mohajan and H. K. Mohajan, Obesity and Its Related Diseases: A New Escalating Alarming in Global Health, *Journal of Innovations in Medical Research*, 2023, **2**, 12–23.

6 E. D. Parker, J. Lin, T. Mahoney, N. Ume, G. Yang, R. A. Gabbay, N. A. Elsayed and R. R. Bannuru, Economic Costs of Diabetes in the U.S. in 2022, *Diabetes Care*, 2024, **47**, 26–43.

7 J. R. Bober and N. U. Nair, Galactose to tagatose isomerization at moderate temperatures with high conversion and productivity, *Nature Communications 2019 10:1*, 2019, **10**, 4548-.

8 A. Ahmed, T. A. Khan, D. D. Ramdath, C. W. C. Kendall and J. L. Sievenpiper, Rare sugars and their health effects in humans: a systematic review and narrative synthesis of the evidence from human trials, *Nutr. Rev.*, 2021, **80**, 255.

9 A. Smith, A. Avery, R. Ford, Q. Yang, A. Goux, I. Mukherjee, D. C. A. Neville and P. Jethwa, Rare sugars: metabolic impacts and mechanisms of action: a scoping review, *Br. J. Nutr.*, 2021, **128**, 389.

10 D. Dai and Y. S. Jin, Rare sugar bioproduction: advantages as sweeteners, enzymatic innovation, and fermentative frontiers, *Curr. Opin. Food Sci.*, 2024, **56**, 101137.

11 M. Guerrero-Wyss, S. Durán Agüero and L. Angarita Dávila, D-Tagatose Is a Promising Sweetener to Control Glycaemia: A New Functional Food, *Biomed Res. Int.*, DOI:10.1155/2018/8718053.

12 J. Jayamuthunagai, P. Gautam, G. Srisowmeya and M. Chakravarthy, Biocatalytic production of D-tagatose: A potential rare sugar with versatile applications, *Crit. Rev. Food Sci. Nutr.*, 2017, **57**, 3430–3437.

13 D. D. Torrico, J. Tam, S. Fuentes, C. G. Viejo and F. R. Dunshea, D-Tagatose as a Sucrose Substitute and Its Effect on the Physico-Chemical Properties and Acceptability of Strawberry-Flavored Yogurt, *Foods*, 2019, **8**, 256.

14 Y. Lu, G. V. Levin and T. W. Donner, Tagatose, a new antidiabetic and obesity control drug, *Diabetes Obes. Metab.*, 2008, **10**, 109–134.

15 H. Zhang, X. Mao, Z. Lu, C. Gao, Z. Chen and J. Liu, Advances in Biological Production of D-Tagatose: A Comprehensive Overview, *Fermentation 2025, Vol. 11,* DOI:10.3390/FERMENTATION11020046.

16 P. Miao, Q. Wang, K. Ren, Z. Zhang, T. Xu, M. Xu, X. Zhang and Z. Rao, Advances and Prospects of d-Tagatose Production Based on a Biocatalytic Isomerization Pathway, *Catalysts 2023, Vol. 13,* DOI:10.3390/CATAL13111437.

17 S. Babaei, N. Arabi, X. Shi, G. W. Huber, E. Camprubi and J. Zhao, Sustainable Production of Low-Calorie Tagatose via CaO-Promoted Galactose Isomerization with CO2Neutralization under Ambient Conditions, *Ind. Eng. Chem. Res.*, 2025, **64**, 18656–18663.

18 J. R. Beadle, J. P. Saunders and T. J. Wajda, Process for manufacturing tagatose.

19 Khoiruddin, I. N. Widiasa and I. G. Wenten, Removal of inorganic contaminants in sugar refining process using electrodeionization, *J. Food Eng.*, 2014, **133**, 40–45.

20 M. Coca, M. T. García, G. González, M. Peña and J. A. García, Study of coloured components formed in sugar beet processing, *Food Chem.*, 2004, **86**, 421–433.

21 A. M. Dehkordi, M. S. Tehrany and I. Safari, Kinetics of Glucose Isomerization to Fructose by Immobilized Glucose Isomerase (Sweetzyme IT, *Ind. Eng. Chem. Res.*, 2009, **48**, 3271–3278.

22 P. Kim, Current studies on biological tagatose production using L-arabinose isomerase: a review and future perspective, *Appl. Microbiol. Biotechnol.*, 2004, **65**, 243–249.
23 D. K. Oh, Tagatose: properties, applications, and biotechnological processes, *Appl. Microbiol. Biotechnol.*, 2007, **76**, 1–8.
24 Z. Xu, S. Li, X. Feng, J. Liang and H. Xu, L-Arabinose isomerase and its use for biotechnological production of rare sugars, *Appl. Microbiol. Biotechnol.*, 2014, **98**, 8869–8878.
25 A. Muñoz-Labrador, R. Lebrón-Aguilar, J. E. Quintanilla-López, P. Galindo-Iranzo, S. M. Azcarate, S. Kolida, V. Kachrimanidou, V. Garcia-Cañas, L. Methven, R. A. Rastall, F. J. Javier Moreno and O. Hernandez-Hernandez, Prebiotic Potential of a New Sweetener Based on Galactooligosaccharides and Modified Mogrosides, *J. Agric. Food Chem.*, 2022, **70**, 9048–9056.
26 L. N. Bell, Tagatose Stability in Beverages as Impacted by Composition and Thermal Processing, *Processing and Impact on Active Components in Food*, 2014, 619–627.
27 I. H. Cho, S. Lee, H. R. Jun, H. J. Roh and Y. S. Kim, Comparison of volatile Maillard reaction products from tagatose and other reducing sugars with amino acids, *Food Sci. Biotechnol.*, 2010, **19**, 431–438.
28 G. V. Levin, Tagatose, the new GRAS sweetener and health product, *J. Med. Food*, 2002, **5**, 23–36.
29 Y. Lu, G. Wang, W. He, Y. Sun and M. Wang, A synergistic strategy coupling enzymatic isomerization with boronate affinity adsorption for efficient tagatose biosynthesis, *Bioresour. Technol.*, 2026, **445**, 134042.
30 J. Zhao, Z. Wang, Q. Jin, D. Feng and J. Lee, Isomerization of Galactose to Tagatose: Recent Advances in Non-enzymatic Isomerization, *J. Agric. Food Chem.*, 2023, **71**, 4228–4234.
31 T. R. James Beadle, J. P. Saunders and T. J. Wajda, Process for manufacturing tagatose.
32 J. Zhao, E. Cruz, X. Shi, S. A. Rankin and G. W. Huber, Production of Tagatose from Galactose with CaO at Room Temperature, *ChemCatChem*, DOI:10.1002/CCTC.202401533.
33 Tagatose production using simulated moving bed separation.
34 N. Kim, J. Jeon, R. Chen and X. Su, Electrochemical separation of organic acids and proteins for food and biomanufacturing, DOI:10.1016/j.cherd.2021.12.009.
35 J. S. White, Sucrose, HFCS, and Fructose: History, Manufacture, Composition, Applications, and Production, *Fructose, High Fructose Corn Syrup, Sucrose and Health*, 2014, 13–33.
36 K. Hashimoto, K. Sakaguchi, R. Kono, S. Adachi and Y. Watanabe, Isomerization and epimerization of galactose using an anion exchange resin, *Food and Bioproducts Processing*, 2025, **150**, 151–158.
37 T. Preechakun, S. Pongchaiphol, V. Champreda, N. Laosiripojana and M. Raita, Separation of xylose and xylooligosaccharides from sugarcane trash extracted from hydrothermal process and followed by ion-exchange resin technique, *Biomass Bioenergy*, 2025, **197**, 107826.
38 R. G. M. van der Sman and S. Renzetti, Understanding functionality of sucrose in biscuits for reformulation purposes, *Crit. Rev. Food Sci. Nutr.*, 2019, **59**, 2225–2239.
39 L. El Hosry, V. Elias, V. Chamoun, M. Halawi, P. Cayot, A. Nehme and E. Bou-Maroun, Maillard Reaction: Mechanism, Influencing Parameters, Advantages, Disadvantages, and Food Industrial Applications: A Review, *Foods*, 2025, **14**, 1881.
40 M. L. Heermann, J. Brown, K. J. K. Getty and U. Yucel, Assessing Functionality of Alternative Sweeteners in Rolled “Sugar” Cookies, *Processes 2022, Vol. 10,* DOI:10.3390/PR10050868.
41 N. Dragomir, D. M. Grigore and E. N. Pogurschi, Beyond Sugar: A Holistic Review of Sweeteners and Their Role in Modern Nutrition, *Foods*, 2025, **14**, 3182.
42 A. De Vivo, A. Balivo, F. Esposito, R. Romano, T. Cirillo, F. Sarghini and A. Genovese, Mitigation of acrylamide in cookies through partial replacement of conventional sugars with erythritol and maltitol, *Food Chem.*, 2026, **512**, 148821.
43 M. Grembecka, Sugar alcohols—their role in the modern world of sweeteners: a review, *European Food Research and Technology*, 2015, **241**, 1–14.
44 E. McKenzie and S. Y. Lee, Sugar reduction methods and their application in confections: a review,

Food Sci. Biotechnol., 2022, **31**, 387.
45 L. N. Bell, Tagatose Stability Issues in Food Systems, *Reference Series in Phytochemistry*, 2018, 575–589.
46 Effects of Various Sugars Including Tagatose and Their Molar Concentrations on the Maillard Browning Reaction, https://www.researchgate.net/publication/263992830_Effects_of_Various_Sugars_Including_Tagatose_and_Their_Molar_Concentrations_on_the_Maillard_Browning_Reaction, (accessed 9 April 2026).
47 E. Timmermans, A. Bautil, K. Brijs, I. Scheirlinck, R. Van der Meulen and C. M. Courtin, Sugar Levels Determine Fermentation Dynamics during Yeast Pastry Making and Its Impact on Dough and Product Characteristics, *Foods*, 2022, **11**, 1388.
48 M. Starowicz, A. Ostaszyk and H. Zieliński, The Relationship between the Browning Index, Total Phenolics, Color, and Antioxidant Activity of Polish-Originated Honey Samples, *Foods*, 2021, **10**, 967.
49 M. Guerrero-Wyss, S. Durán Agüero and L. Angarita Dávila, D-Tagatose Is a Promising Sweetener to Control Glycaemia: A New Functional Food, *Biomed Res. Int.*, 2018, **2018**, 8718053.
50 A. de C. Ortiz, S. O. M. Fideles, C. H. B. Reis, B. T. Pagani, L. M. M. Bueno, M. B. M. Moscatel, R. L. Buchaim and D. V. Buchaim, D-Tagatose: A Rare Sugar with Functional Properties and Antimicrobial Potential against Oral Species, *Nutrients*, DOI:10.3390/NU16121943.
51 H. Zhang, X. Mao, Z. Lu, C. Gao, Z. Chen and J. Liu, Advances in Biological Production of D-Tagatose: A Comprehensive Overview, *Fermentation 2025, Vol. 11,* DOI:10.3390/FERMENTATION11020046.
52 D. Dai and Y. S. Jin, Rare sugar bioproduction: advantages as sweeteners, enzymatic innovation, and fermentative frontiers, *Curr. Opin. Food Sci.*, 2024, **56**, 101137.
53 A. Muñoz-Labrador, R. Lebrón-Aguilar, J. E. Quintanilla-López, P. Galindo-Iranzo, S. M. Azcarate, S. Kolida, V. Kachrimanidou, V. Garcia-Cañas, L. Methven, R. A. Rastall, F. J. Javier Moreno and O. Hernandez-Hernandez, Prebiotic Potential of a New Sweetener Based on Galactooligosaccharides and Modified Mogrosides, *J. Agric. Food Chem.*, 2022, **70**, 9048–9056.
54 Y. Lu, G. Wang, W. He, Y. Sun and M. Wang, A synergistic strategy coupling enzymatic isomerization with boronate affinity adsorption for efficient tagatose biosynthesis, *Bioresour. Technol.*, 2026, **445**, 134042.
55 P. Miao, Q. Wang, K. Ren, Z. Zhang, T. Xu, M. Xu, X. Zhang and Z. Rao, Advances and Prospects of d-Tagatose Production Based on a Biocatalytic Isomerization Pathway, *Catalysts 2023, Vol. 13,* DOI:10.3390/CATAL13111437.
56 J. Zhao, Z. Wang, Q. Jin, D. Feng and J. Lee, Isomerization of Galactose to Tagatose: Recent Advances in Non-enzymatic Isomerization, *J. Agric. Food Chem.*, 2023, **71**, 4228–4234.
57 T. R. James Beadle, J. P. Saunders and T. J. Wajda, United States Patent (19) Beadle et al. 54 PROCESS FOR MANUFACTURING.
58 J. R. Beadle, J. P. Saunders and T. J. Wajda, United States Patent (19) Beadle et al. (54) (75) (73) 21 (22) (62) (51) (52) (58) PROCESS FOR MANUFACTURING TAGATOSE.
59 Tagatose production from deproteinized whey and purification by continuous chromatography.
60 N. Kim, J. Jeon, R. Chen and X. Su, Electrochemical separation of organic acids and proteins for food and biomanufacturing, DOI:10.1016/j.cherd.2021.12.009.
61 Khoiruddin, I. N. Widiasa and I. G. Wenten, Removal of inorganic contaminants in sugar refining process using electrodeionization, *J. Food Eng.*, 2014, **133**, 40–45.
62 S. Babaei, N. Arabi, X. Shi, G. W. Huber, E. Camprubi and J. Zhao, Sustainable Production of Low-Calorie Tagatose via CaO-Promoted Galactose Isomerization with CO2Neutralization under Ambient Conditions, *Ind. Eng. Chem. Res.*, 2025, **64**, 18656–18663.
63 T. Preechakun, S. Pongchaiphol, V. Champreda, N. Laosiripojana and M. Raita, Separation of xylose and xylooligosaccharides from sugarcane trash extracted from hydrothermal process and followed by

ion-exchange resin technique, *Biomass Bioenergy*, 2025, **197**, 107826.
64 X. fang Chen, H. long Li, X. ran Ji, Z. jie Shen, H. jun Guo, S. miao Yao, M. kun Wang, L. Xiong and X. de Chen, Preparation, separation and purification of 5-hydroxymethylfurfural from sugarcane molasses by a self-synthesized hyper-cross-linked resin, *Sep. Purif. Technol.*, DOI:10.1016/J.SEPPUR.2023.123661.
65 W. Chomchuen, L. Simasatitkul, W. Mens, S. Jantasee and C. Chaiya, Sustainable conversion of bagasse into porous carbon using industrial excess heat and steam: Syrup decolorization and techno-economic analysis, *Results in Engineering*, 2025, **25**, 103705.
66 P. I. Omwene, Z. B. O. Sarihan, A. Karagunduz and B. Keskinler, Bio-based succinic acid recovery by ion exchange resins integrated with nanofiltration/reverse osmosis preceded crystallization, *Food and Bioproducts Processing*, 2021, **129**, 1–9.
67 X. Wen, H. Lin, G. Liu, Y. Ning, Y. Ren, C. Li, C. Zhang, N. Dong, J. Lin, X. Song, G. Zhuang and J. Lin, D-tagatose biotransformation from lactose by lactase and recombinant Bacillus subtilis expressing l-arabinose isomerase, and the product separation, purification and crystallization, *Food Microbiol.*, DOI:10.1016/J.FM.2025.104785.
68 X. Wen, H. Lin, G. Liu, Y. Ning, X. Xu, H. Hu, Y. Ren, C. Li, C. Zhang, N. Dong, X. Song, J. Lin and J. Lin, Eco-friendly production, separation and purification of D-tagatose and D-allulose from whey powder via one-pot whole-cells biotransformation, yeast fermentation and chromatography, *Food Res. Int.*, DOI:10.1016/J.FOODRES.2025.116109.
69 K. Hashimoto, K. Sakaguchi, R. Kono, S. Adachi and Y. Watanabe, Isomerization and epimerization of galactose using an anion exchange resin, *Food and Bioproducts Processing*, 2025, **150**, 151–158.
70 New Numbers for GS2 White Sugar Methods - ICUMSA, https://www.icumsa.org/new-numbering-system/new-numbers-for-gs2-white-sugar-methods/, (accessed 10 November 2025).
71 İ. B. Can, Ö. Bıçak, S. Özçelik, M. Can and Z. Ekmekçi, Sulphate Removal from Flotation Process Water Using Ion-Exchange Resin Column System, *Minerals 2020, Vol. 10,* 2020, **10**, 1–17.
72 Ion Exchange - Friedrich G. Helfferich - Google Books, https://books.google.com/books?id=F9OQMEA88CAC&printsec=frontcover#v=onepage&q&f=false, (accessed 11 January 2026).
73 J. S. White, Straight talk about high-fructose corn syrup: what it is and what it ain't, *Am. J. Clin. Nutr.*, DOI:10.3945/AJCN.2008.25825B.
74 Handbook of Starch Hydrolysis Products and their Derivatives, *Handbook of Starch Hydrolysis Products and their Derivatives*, DOI:10.1007/978-1-4615-2159-4.
75 J. Małecki, I. Tomasevic and B. G. Sołowiej, The Influence of the Syrup Type on Rheology, Color Differences, Water Activity, and Nutritional and Sensory Aspects of High-Protein Bars for Sportsmen, *J. Food Qual.*, 2022, **2022**, 2317676.
76 Measurement and Calculation of the Electrical Conductivity of Model Honey Solutions, https://www.researchgate.net/publication/292608070_Measurement_and_Calculation_of_the_Electrical_Conductivity_of_Model_Honey_Solutions, (accessed 13 January 2026).
77 ICUMSA Method GS2-17 (2011) - ICUMSA, https://www.icumsa.org/methods/icumsa-method-gs2-17-2011/, (accessed 14 January 2026).
78 ISO 11885:2007 - Water quality - Determination of selected elements by inductively coupled plasma optical emission spectrometry (ICP-OES), https://webstore.ansi.org/standards/iso/iso118852007, (accessed 15 January 2026).
79 ISO 24683:2022 - High fructose syrup — Specifications and test methods, https://www.iso.org/standard/79431.html, (accessed 14 January 2026).
80 L. M. Hanover and J. S. White, Manufacturing, composition, and applications of fructose, *Am. J. Clin. Nutr.*, 1993, **58**, 724S-732S.
81 ICUMSA Method GS2-9 (2024) - ICUMSA, https://www.icumsa.org/methods/icumsa-method-gs2-9-2024/?utm_source=chatgpt.com, (accessed 16 January 2026).

82 J. Liu, P. Wan, C. Xie and D. W. Chen, Membrane filtration without adding lime water combined with vacuum heating enhances green odor in brown sugar processing, *LWT*, 2023, **182**, 114834.
83 K. Julai, P. Sridonpai, C. Ngampeerapong, K. Tongdonpo, U. Suttisansanee, W. Kriengsinyos, N. On-Nom and N. Tangsuphoom, Effects of Extraction and Evaporation Methods on Physico-Chemical, Functional, and Nutritional Properties of Syrups from Barhi Dates (Phoenix dactylifera L.), *Foods*, 2023, **12**, 1268.
84 Corn Sweetener | Refining | Ion Exchange Resins | Ecolab, https://www.purolite.com/index/core-technologies/industry/food-and-beverage/sweetener-applications/corn-sweetener-refining-with-ion-exchange-resins?utm_source=chatgpt.com, (accessed 16 January 2026).
85 Ion Exchange in the Sugar Industry.
86 Food Processing - Fructose/Glucose, https://www.puritech.be/food-processing/fructose-glucose/, (accessed 16 January 2026).
87 M. Gupta, S. Kapoor, M. Bala, B. Vipin and C. Mahajan, Quality Characteristics and Storage Stability of Guava Nectar Formulated with Natural Sweeteners, *Food Technol. Biotechnol.*, 2025, **63**, 480–492.
88 M. C. Brinkman, A. A. Teferra, N. O. Kassem and N. O. F. Kassem, Effect of electric heating and ice added to the bowl on mainstream waterpipe semivolatile furan and other toxicant yields, *Tob. Control*, 2019, **29**, S110–S116.
89 B. Fallico, E. Arena and M. Zappala, Degradation of 5-hydroxymethylfurfural in honey, *J. Food Sci.*, DOI:10.1111/j.1750-3841.2008.00946.x.
90 S. Krainer, R. Brodschneider, J. Vollmann, K. Crailsheim and U. Riessberger-Gallé, Effect of hydroxymethylfurfural (HMF) on mortality of artificially reared honey bee larvae (Apis mellifera carnica), *Ecotoxicology*, 2016, **25**, 320–328.
91 B. W. LeBlanc, G. Eggleston, D. Sammataro, C. Cornett, R. Dufault, T. Deeby and E. S. Cyr, Formation of hydroxymethylfurfural in domestic high-fructose corn syrup and its toxicity to the honey bee (Apis mellifera), *J. Agric. Food Chem.*, 2009, **57**, 7369–7376.
92 A. A. Asiz, PHYSICOCHEMICAL AND STRUCTURAL OPTIMIZATION OF DATE (Phoenix dactylifera L.) SYRUP: IMPACT OF EXTRACTION TEMPERATURES AND PECTIN ADDITION, *Theses*.
93 N. Arabi, S. Babaei, J. Qi, S. Arvelli and J. Zhao, A review of 5-hydroxymethylfurfural production from fructose using heterogeneous catalysts, *Biomass Futures*, 2026, **1**, 100009.
94 U. M. Shapla, M. Solayman, N. Alam, M. I. Khalil and S. H. Gan, 5-Hydroxymethylfurfural (HMF) levels in honey and other food products: effects on bees and human health, *Chem. Cent. J.*, 2018, **12**, 35.
95 J. Małecki, I. Tomasevic and B. G. Sołowiej, The Influence of the Syrup Type on Rheology, Color Differences, Water Activity, and Nutritional and Sensory Aspects of High-Protein Bars for Sportsmen, *J. Food Qual.*, DOI:10.1155/2022/2317676.
96 M. Starzak, M. M.- Zuckerindustrie and undefined 2002, Water activity in concentrated sucrose solutions and its consequences for the availability of water in the film of syrup surrounding the sugar crystal, *researchgate.net*.
97 M. Sramek, B. Woerz, H. Horn, J. Weiss and R. Kohlus, Inactivation kinetics of invertase in honey and honey–glucose syrup formulations: effects of temperature and water activity, *J. Sci. Food Agric.*, 2017, **97**, 1178–1184.
98 US12180553B2 - Tagatose and galactose syrup - Google Patents, https://patents.google.com/patent/US12180553B2/en, (accessed 17 January 2026).
99 Z. Shi, W. Zhu, Z. Lei, X. Yan, X. Zhang, S. Wei and Q. Wang, Intake of Added Sugar from Different Sources and Risk of All-Cause Mortality and Cardiovascular Diseases: The Role of Body Mass Index, *J. Nutr.*, 2024, **154**, 3457–3464.
100 J. M. Rippe and T. J. Angelopoulos, Relationship between Added Sugars Consumption and Chronic

Disease Risk Factors: Current Understanding, *Nutrients*, 2016, **8**, 697.
101 L. Te Morenga, S. Mallard and J. Mann, Dietary sugars and body weight: systematic review and meta-analyses of randomised controlled trials and cohort studies, *BMJ*, DOI:10.1136/BMJ.E7492.
102 Q. Yang, Z. Zhang, E. W. Gregg, W. D. Flanders, R. Merritt and F. B. Hu, Added sugar intake and cardiovascular diseases mortality among US adults, *JAMA Intern. Med.*, 2014, **174**, 516–524.
103 World Health Organization, Guideline. WHO suggests a further reduction of the intake of free sugars to below 5% of total energy intake, *World Health Organization*, 2015, 59.
104 H. Onyeaka, O. Nwaiwu, K. C. Obileke, T. Miri and Z. T. Al-Sharify, Global nutritional challenges of reformulated food: A review, *Food Sci. Nutr.*, 2023, **11**, 2483.
105 J. C. Y. Louie, Sugar Reformulation in Solid Foods: Limitations and Challenges, *Nutr. Bull.*, 2025, **50**, 345.
106 I. H. O. de Lima, N. L. H. Brito, F. A. R. Cardoso and R. H. B. Fuchs, Sensory Characterization of Cookies With Sugar Replacement by Sweeteners Using the Check-All-That-Apply (CATA) Method, *J. Food Sci.*, 2026, **91**, e70888.
107 E. McKenzie and S. Y. Lee, Sugar reduction methods and their application in confections: a review, *Food Sci. Biotechnol.*, 2022, **31**, 387.
108 A. Ahmed, T. A. Khan, D. D. Ramdath, C. W. C. Kendall and J. L. Sievenpiper, Rare sugars and their health effects in humans: a systematic review and narrative synthesis of the evidence from human trials, *Nutr. Rev.*, 2021, **80**, 255.
109 A. Smith, A. Avery, R. Ford, Q. Yang, A. Goux, I. Mukherjee, D. C. A. Neville and P. Jethwa, Rare sugars: metabolic impacts and mechanisms of action: a scoping review, *Br. J. Nutr.*, 2021, **128**, 389.
110 L. N. Bell, Tagatose Stability in Beverages as Impacted by Composition and Thermal Processing, *Processing and Impact on Active Components in Food*, 2014, 619–627.
111 G. V. Levin, Tagatose, the new GRAS sweetener and health product, *J. Med. Food*, 2002, **5**, 23–36.
112 A. de C. Ortiz, S. O. M. Fideles, C. H. B. Reis, B. T. Pagani, L. M. M. Bueno, M. B. M. Moscatel, R. L. Buchaim and D. V. Buchaim, D-Tagatose: A Rare Sugar with Functional Properties and Antimicrobial Potential against Oral Species, *Nutrients*, 2024, **16**, 1943.
113 N. Arabi, S. Babaei, J. Qi, S. Arvelli, S. Janbazialamdari and J. Zhao, Production of tagatose-rich syrup with ion-exchange resin purification, *Sustainable Food Technology*, DOI:10.1039/D6FB00038J.
114 P. B. Pathare, U. L. Opara and F. A. J. Al-Said, Colour Measurement and Analysis in Fresh and Processed Foods: A Review, *Food Bioproc. Tech.*, 2013, **6**, 36–60.
115 S. Ryu, H. Roh, B. Noh, S. Kim, D. Oh, W.-J. Lee, J. Yoon and S.-S. Kim, Effects of Various Sugars Including Tagatose and Their Molar Concentrations on the Maillard Browning Reaction, *Korean Journal of Food Science and Technology*.
116 I. H. Cho, S. Lee, H. R. Jun, H. J. Roh and Y. S. Kim, Comparison of volatile Maillard reaction products from tagatose and other reducing sugars with amino acids, *Food Sci. Biotechnol.*, 2010, **19**, 431–438.
117 A. M. Gomez-Betancur, S. Lignou, B. Pinarli, V. Norton and J. Rodriguez-Garcia, Effect of rare sugars on physical and sensory properties of doughs and biscuits, *Food Hydrocolloids for Health*, 2025, **8**, 100230.
118 B. Pareyt and J. A. Delcour, The role of wheat flour constituents, sugar, and fat in low moisture cereal based products: a review on sugar-snap cookies, *Crit. Rev. Food Sci. Nutr.*, 2008, **48**, 824–839.
119 S. I. F. S. Martins, W. M. F. Jongen and M. A. J. S. Van Boekel, A review of Maillard reaction in food and implications to kinetic modelling, *Trends Food Sci. Technol.*, 2000, **11**, 364–373.
120 O. Rojo-Poveda, L. Barbosa-Pereira, D. Orden, C. Stévigny, G. Zeppa and M. Bertolino, Physical Properties and Consumer Evaluation of Cocoa Bean Shell-Functionalized Biscuits Adapted for Diabetic Consumers by the Replacement of Sucrose with Tagatose, *Foods 2020, Vol. 9,* DOI:10.3390/FOODS9060814.

121 V. Rauh and Y. Xiao, The shelf life of heat-treated dairy products, *Int. Dairy J.*, DOI:10.1016/j.idairyj.2021.105235.
122 S. Chevallier, P. Colonna, G. Della Valle and D. Lourdin, Contribution of major ingredients during baking of biscuit dough systems, *J. Cereal Sci.*, 2000, **31**, 241–252.
123 D. D. Torrico, J. Tam, S. Fuentes, C. G. Viejo and F. R. Dunshea, D-Tagatose as a Sucrose Substitute and Its Effect on the Physico-Chemical Properties and Acceptability of Strawberry-Flavored Yogurt, *Foods*, 2019, **8**, 256.
124 T. P. Labuza and B. Altunakar, Water Activity Prediction and Moisture Sorption Isotherms, *Water Activity in Foods: Fundamentals and Applications*, 2008, 109–154.